On Equivalent Granular Void Ratio and Steady State Behaviour of Loose Sand with Fines

Md. M. Rahman, S. R. Lo and C. T. Gnanendran

1. Md. Mizanur Rahman
   PhD Student
   University of New South Wales, ADFA Campus, Canberra, Australia
   Email: mmrahman@adfa.edu.au; Fax: +61-2-62688337

2. S.R. Robert Lo
   Associate Professor
   University of New South Wales, ADFA Campus, Canberra, Australia
   Email: rlo@adfa.edu.au; Fax: +61-2-62688337

3. C. T. Gnanendran
   Senior Lecturer
   University of New South Wales, ADFA Campus, Canberra, Australia
   Email: r.gnanendran@adfa.edu.au; Fax: +61-2-62688337

Abstract:

Void ratio has traditionally, been used as a state variable for predicting the liquefaction behaviour of soils under the Critical State Soil Mechanics framework. Recent publications show that void ratio may not be a good parameter for characterizing sand with fines. An alternative state variable referred to as equivalent granular void ratio has been proposed to resolve this problem. To calculate this alternative state variable, a *b*-parameter is needed. This *b*-parameter represents the fraction of fines that actively participate in the force structure of the solid skeleton. However, predicting the "*b*" value is problematic. Most, if not all, of the *b*-values reported were determined by case-specific back-analysis, that is, the *b*-value was selected so that a single correlation between equivalent granular void ratio and the measured steady state strength (or cyclic resistance) could be achieved. This paper examines the factors affecting the "*b*" value based on published work on binary packing. This leads to a simple semi-empirical equation for predicting the value of "*b*" based on fines size and fines content. Published data appears to be in support of the proposed equation. A series of experiments were conducted on a specially designed sand-fines type in order to provide additional validation of the proposed equation and to reinforce the use of equivalent granular void ratio in a more generalized context.

KEY WORDS:

Void ratio, state variable, Steady State, Critical State, liquefaction

1. Introduction

Early laboratory studies on liquefaction were mainly on clean sand although the occurrence of loose sand with fines is not uncommon. It has been understood, since the 1960's, that the presence of fines in some manner affects liquefaction behaviour. Some recent studies showed a decrease in liquefaction resistance with addition of fines up to a limiting fines content, but followed by an increase in liquefaction resistance with further increase in fines (Altun et al. 2005; Thevanayagam 1998; Xenaki and Athanasopoulos 2003; Yang et al. 2006). However, the prediction of these behaviours under the Critical State Soil Mechanics presents special challenges. The Steady State (SS) or Critical State (CS) line/curve is dependent of fines content. The term Steady State Line will be used hereafter even though it may be a curve.

One of the possible reasons that lead to the lack of a single Steady State Line may be due to the use of void ratio as a state variable. This is because of the non-active participation of fines in the force structure of a sand-fines mixture. To resolve this problem, a new state variable referred to as intergranular void ratio was proposed by considering the non-active fines as voids. It has been suggested that the intergranular void ratio should be used instead of void ratio for low fines content (Georgiannou et al. 1990; Georgiannou et al. 1991; Hight and Georgiannou 1995; Kuerbis et al. 1988; Ovando-Shelley and Pérez 1997, Thevanayagam 1998). However, intergranular void ratio is not applicable at higher fines content (Ni et al. 2006; Ni et al. 2004; Thevanayagam 2000; Yang et al. 2006a; 2006b). Thevanayagam (2000) introduced the concept of equivalent granular void ratio for higher fines content and this approach requires an additional parameter "*b*" that presents the fraction of fines participating in the force structure of the solid skeleton. However, the prediction of *b*-value is a problematic and controversial issue (Ni et al. 2004; Thevanayagam 2001). Most, if not all, of the reported *b*-values are determined so that the Steady State strength or cyclic resistance for a given sand-fines type can be correlated to equivalent granular void ratio irrespective of fines content. This means these values are case specific back-analyzed values rather

than predicted values. An in-depth discussion of the challenges in the determination of *b*-values is given in the Literature Review Section.

The broad objective of this paper is to examine the physical basis of equivalent granular void ratio and the "*b*" parameter so that a more general method for predicting the equivalent granular void ratio can be established. Equivalent granular void ratio rather than the simpler inter-granular void ratio is used as the state variable because the former is a more general concept. This necessitates the development of a semi-empirical, yet physically reasonable, equation for predicting the *b*-value for a range of sand-fines types. The performance of the proposed equation was first evaluated with a number of published data sets available. It was then validated with test results obtained from a specially designed testing program. This allows the study of the behaviour of sand with fines with the Critical State Soil Mechanics (CSSM) framework and using a single Steady State Line (hereafter abbreviated as SSL) with the equivalent granular void ratio as the alternative state variable.

2. Literature Review

2.1 Intergranular void ratio

Mitchell (1976) pointed out the non-active role of fines in a granular phase structure and used such concept to determine the amount of non-active clay content. Kenney (1977) found that a clayey sand with a combined fines and water content of less than 40% to 50% by volume had a residual strength close to that of the host sand with a void space same as that occupied by the fines plus water. Troncoso and Verdugo (1985) also reported similar findings in relation to liquefaction resistance of tailing sand with up to 30% silty fines. Though these publications support the concept of intergranular void ratio, that is the fines occupying the pore space of the host granular material are non-active, Kuerbis et al. (1988) may be the first comprehensive published work that used intergranular void ratio as the comparison basis for undrained shear strength behaviour. Their paper suggested that fines simply occupied the voids in the sand skeleton and

therefore the behaviour was controlled by sand skeleton only. Thus, by neglecting the fines, they proposed the use of a sand skeleton void ratio calculated by Eqn (1) below.

[1] $$e_{skeleton} = \frac{V_T G_S \rho_W - (M - M_f)}{(M - M_f)}$$

where $e_{skeleton}$ = sand skeleton void ratio, V_T = total volume of soil sample, G_s = specific gravity of soil, ρ_w = density of water, M = mass of soil, M_f = mass of fines. The sand skeleton void ratio is in fact the intergranular void ratio. This paper reported that the measured cyclic resistance behaviour at the same intergranular void ratio were similar. Georgiannou et al. (1990), in studying the behaviour of a clayey sand (Ham River Sand), proposed the use of intergranular void ratio, e_g, calculated by:

[2] $$e_g = \frac{\text{Volume of voids} + \text{volume of clay}}{\text{volume of granular phase}}$$

They observed that different specimens of similar intergranular void ratio manifested essentially identical effective stress paths in anisotropically consolidated undrained compression triaxial tests. Thevanayagam (1998) found that the Steady States of a sand with non-plastic fines, when plotted in the intergranular void versus mean effective stress space are located close to a single line/curve irrespective of fines content. He calculated intergranular void ratio, e_g , with Eqn (3) below.

[3] $$e_g = \frac{e + f_c}{1 - f_c}$$

Where, e = void ratio and f_c = fines content in decimal. Though different researcher used different equation for intergranular void ratio, Chu and Leong (2002) showed that the apparently different equations used for calculating intergranular void ratio are essentially identical. However, the definition of intergranular void ratio by assuming that fines are completely non-active is not universally applicable for the entire range of fines content.

With increasing fines content, fines may come in between the contact of sand grains and participate in the force structure. Some initially non-active fines may also

become part of the form chain as a result of the movements of soil during shearing. A more general concept is to have a fraction of the fines actively participating in the force structure. To take into such a mechanism, Thevanayagam et al. (2000) proposed the concept of equivalent granular void ratio, which was also referred to as intergranular contact index void ratio, e^*, defined as:

[4] $$e^* = \frac{e + (1-b) f_c}{1 - (1-b) f_c}$$

The physical meaning of "b" is the fraction of fines which actively participates in the force structure. The rationale behind Eqn (4) requires a fines-in-sand model (Thevanayagam 1998) and that $b \geq 0$. Eqn (4) may be considered as a generalization of Eqn (3). When $b = 0$, it reduces to the earlier equations that assumes all the fines are non-active. Therefore e_g as defined by Eqn (3) may be considered as an approximation of e^* at low fines content. This is consistent with the finding that e_g may be an adequate concept for low fines content (Thevanayagam 1998, Georgianou et al. 1990,1991), and that Yang et al. (2006b) referred e^* as corrected intergranular void ratio. A gradual increase in contribution of fines in the force structure can be reflected by setting "b" in the range of 0 to 1. The successful application of e^* has been discussed in the literature by Ni et al. (2006; 2004), Thevanayagam (2000) and Yang et al. (2006a). It is pertinent to note that e^* as defined by Eqn (4) has also been referred to by different names in the literature: as granular void ratio equivalent, contact index void ratio, equivalent intergranular contact index void ratio, equivalent intergranular contact index, granular void ratio equivalent and equivalent granular void ratio. For simplicity, the last term "equivalent granular void ratio" will be used in this paper.

However, the prediction of the "b" value, and thus the determination of equivalent granular void ratio, is a problematic and controversial issue. Most researchers assumed "b" is independent of fines content and determined "b" for a given sand-fines type by a back-analysis process, i.e. to target a single correlation (irrespective of fines content) between the behaviour studied and the equivalent granular void ratio. Thevanayagam and Martin (2002) reported that $b = 0.35$ for Ottawa sand-silt mix and Ni et al. (2004)

reported $b = 0.25$ for Toyoura sand-silt mix. Thevanayagam (2001) and Thevanayagam et al. (2002a) suggested that "b" depends on $U_c U_f^2/\chi_T$, where U_c = uniformity coefficient of coarse matrix, U_f = uniformity coefficient of fines and χ_T is the diameter ratio defined as D_{50}/d_{50}, where D is the diameter of the coarser matrix and d is the diameter of the fines and subscript "50" denotes the median value. Ni et al. (2004; 2005) suggested that "b" depends on the diameter ratio defined by $\chi = D_{10}/d_{50}$, where subscript "10" denotes 10% lower fractile. They reported $b = 0.7$ for an Old Alluvium sand with 9% non-plastic fines. This is a relatively high b-value for a low fines content. Yang et al. (2006a; 2006b), based on his study on Hokksund sand with Chengbei non-plastic fines, suggested that $b = 0.25$ could be used for fines content up to 20%, but $b = 0.40$ should be used at the threshold fines content of 30%. A b-value independent of fines content does not appear to be consistent with a fines-in-sand model. It is also inconsistent with the mathematical requirement that Eqn (3) is an approximate form of Eqn (4) at low fines content. The determination of b-value by case-specific back-analysis may also lead to a negative b-value (Ni et al. 2004), which is inconsistent with the physical meaning of "b". The above discussion highlighted the need for having a physically reasonable and mathematically consistent equation for predicting b-values. This is an essential step for the determination of equivalent granular void ratio.

2.2 Binary packing

As the "b" parameter was supposedly introduced to reflect the contribution of fines to the force structure, binary packing studies were examined. These studies were mainly reported in the ceramic, concrete and powder technology areas and with the original objective of minimizing storage space or maximising densities. Wickland et al. (2006) showed that binary packing studies can provide a rational basis for the design of waste rock and tailings mixtures. The study of McGeary (1961) on the binary packing of spherical balls is of particular relevance to geotechnical engineering. The densities achieved by different binary packings of spheres, i.e. spheres of two different sizes and relative composition, placed using a special vibratory procedure were measured. The test results showed that if $D/d > 6.5$, where D is the diameter of the larger sphere and d is that of smaller sphere, the experimental density achieved would be close to the theoretical

curve computed based on the smaller spheres all located in the voids between the larger spheres. However, test results for D/d < 4.7 deviated significantly from the theoretical curves thus showing a significant percentage of the smaller spheres were loacted between the larger spheres. Lade et al. (1998) re-analyzed the data of McGeary (1961) and presented the findings in terms of void ratio as shown Fig. 1 of this paper (in a slightly modified format). Irrespective of D/d, the void ratio achieved in McGeary's experiment decreases with fines content until the fines content reaches a threshold value. This threshold fines content, identifiable from the plot as a turning point, defines a point when the packing changes from "fines in a coarse matrix" to that of "coarse material in a matrix of fines". The trend will be reversed with further increase in fines content. The void ratio versus fines content curve thus has a V-shape. For fines content less than the threshold value, the deviation of the experimental curve from the theoretical relationship increases with fines content. This implies an increasing fraction of the fines could not migrate to the void space and were located between the larger spheres. Fig. 2, also reproduced from Lade et al. (1998) with slight formatting modification, showed that variation of the lowest void ratio (achieved in McGeary's experiment) with D/d. Note that this lowest void ratio is that at the threshold fines content. At high size ratio, say D/d > 9, the rate of reduction of the lowest void ratio with increase in D/d was slight and approached asymptotically to the theoretical minimum value inferred from the most efficient packing. This is because D/d only has a slight influence on the migration of the smaller particles into the gap between the larger ones. For small size ratio, say D/d < 6, the lowest void ratio varied rapidly with D/d because some of the smaller particles moved in between the larger ones and opened up the voids between the larger ones adequately for the smaller particles to migrate into. The extent this occurred was dependent on D/d. One can also infer a "bend" delineating these two regimes at D/d ≅ 7. This value is consistent with the geometric calculation of fitting a smaller sphere between larger ones (Lade et al 1998). These findings on binary packing highlight the factors that influence the "extent of contacts" between large and small particles of a binary mix, and thus relevant to the prediction of "*b*".

3 Prediction of "b"-value

3.1 Factors affecting "*b*"–value

The "*b*" value is a measure of the participation of the fines in the force structure. Fines that are between coarse particles are in the force chain whereas fines that are located in the gaps between the coarse grains have little contribution to the force structure. Therefore the factors that affect the void ratio of a binary packing, including the deviation of the V-shape curve from the theoretical curve of Fig. 1, can be used to infer the factors that affect the "*b"* value. Figs. 1 and 2 show that the void ratio of a binary packing is dependent on both the relative composition and the size ratio. Therefore, "*b*" is a function of both f_c and χ. This functional relationship has to possess the following characteristics as inferred from the previous section on binary packing.

- There exists a threshold fines content. When the fines content exceeds a threshold value denoted as f_{thre} hereafter, the fines become the matrix, and the concept of a *b*-value and equivalent granular void ratio ceased to be valid for studying fines in a matrix of coarse materials.
- For fines content less than the threshold value (which is the focus of this paper), the *b*-value increases with fines content (as the deviation of the V-shape curves from the theoretical line of Fig. 1 increases with fines content).
- There exists a narrow zone (with D/d in the range of 6 to 8) where "*b*" changes gradually with fines content. Outside this zone two distinct regimes can be identified.
    - For D/d > 8, "*b*" increases slowly with size ratio.
    - For D/d < 6, "*b*" increases rapidly with reduction in size ratio.

3.2 Prediction equation

In this section, the functional relationship $b = F(\chi, f_c)$ is developed using a semi-empirical approach. For host sand and fines that are not single size, the size of the host sand will be characterized by the lower 10% fractile, D_{10}, whereas that of fines are characterize by d_{50}, the median size. This is in line with the argument of Ni et al. (2004; 2005). Therefore the size ratio, χ, is defined as D_{10}/d_{50}. The "fines in sand" model

implies that the grading curves of the host sand and fines are spaced apart. All the data sets studied in this paper satisfy this requirement.

This function has to be able to simulate the various attributes as discussed in the previous sub-section, and yet has a simple form. Eqn (5) given below satisfies such a requirement.

[5] $$b = \left(1 - e^{-m(f_c)^2/k}\right).\left(\frac{r.f_c}{f_{thre}}\right)^r$$

where $r = \chi^{-1}$ = d/D, $k = (1 - r^{0.25})$, and "*m*" is a fitting constant. It was found that m = 2.5 is satisfactory for a large number of data sets as discussed in a later section. Therefore, Eqn (5) becomes:

[5a] $$b = \left(1 - e^{-2.5(f_c)^2/k}\right).\left(\frac{r.f_c}{f_{thre}}\right)^r$$

Eqn (5a) ensures $b < 1$ as the limiting values of both factors are unity.

The variation of *"b"* with χ, normalized with *b(20)*, is presented in Fig. 3a. Normalized plots are presented so that the *b*-χ plots corresponding to different fines content can be compared. It is evident that the general trend is independent of f_c. For $\chi \leq$ 4.5, this factor changes rapidly with size ratio, but at a higher size ratio, say exceeding 9, "*b*" reduces very slowly with size ratio. The "turning point" may be inferred to be in the range of 6 to 8. These characteristics are in line with those listed in the previous section. This general trend implies that the predicted *b*-value is not sensitive to χ provided $\chi > 8$. However, at smaller size ratio, the input parameter χ has a significant effect on the predicted *b*-value. The general shape of the plots presented in Fig. 3a is attributed to the first factor, i.e. $\left(1 - e^{-2.5(f_c)^2/k}\right)$, of the prediction equation. This is illustrated by the

normalized plots of Fig. 3b. The influence of χ on the value of the first factor is largely achieved through "k". In general, a higher size ratio will give to a higher "k" value, which then leads to a lower value for the first factor.

The second factor $\left(rf_c / f_{thre}\right)^r$ of the equation ensures that $b \rightarrow 0$ as $f_c \rightarrow 0$. Therefore, Eqn (4) for defining e^* degenerates to Eqn (3) for defining e_g. This is consistent with published work showing e_g (calculated with $b = 0$) is an adequate approximation for low fines content.

The resultant variation of "b" with fines content, normalized relative to threshold fines content, is shown in Fig. 3c. The plots showed at low fines content, both the value of "b" and $\partial b / \partial f_c$ are small. This is again consistent with published finding that e_g is an acceptable approximation for low fines content. It also meant that, at low fines content, the predicted b-value is not sensitive to the input parameters f_c and f_{thre}. However, at higher fines content, $\partial b / \partial f_c$ begins to take a significant value. This implies the predicted b-value is dependent on getting reliable values of f_c and f_{thre}.

4. Evaluation of the proposed equation using published data

The proposed equation was evaluated using published data sets by the following methodology:

- The b-values were calculated using Eqn (5a), which could then be substituted into Eqn (4) to yield equivalent granular void ratios.
- It was examined whether a single behaviour trend independent of fines content could be obtained utilizing the equivalent granular void ratio as the alternative state variable.

Two types of behaviour were examined: the Steady State (SS) behaviour from monotonic undrained shearing and the cyclic mobility behaviour from cyclic triaxial testing. In the former case, the desired outcome is to achieve a unique correlation between e^* and p' at SS. In the latter case, the desired outcome is a single correlation between e^* and Cyclic Resistance as defined in Ishihara (1993).

Three input parameters, namely size ratio, fines content and threshold fines content are required in the prediction. The first two parameters were always reported in published literature. In determining the threshold fines content, the original publication was always consulted to avoid confusion between threshold fines content and maximum fines content covered in a testing program. If the threshold fines content was not reported and could not be inferred from published data, the average value of 30% was used.

4.1 Steady State behaviour from monotonic undrained Shearing

The evaluation exercise was conducted on five data sets extracted from published literatures. A brief summary of these data sets is presented in Table 1a, and FC denotes fines content expressed in percentage. It is recognized that visual appearance of scatter may be subjectively influenced by the scale used in plotting, the number of data points and overall pattern of the data points. In order to have an objective assessment, two statistical quantities were calculated for each data set: i) the half-spread of the source data in terms of e, and ii) the root-mean-square-deviation (RMSD) of the (e^*, p'_{SS}) data points from the best-fit trend line/curve. The definition of these two quantities are detailed in Appendix A. The magnitude of RMSD relative to the half-spread of the source data will provide an objective basis to assess whether the influence of fines content was significantly reduced by synthesizing data points in the e^*-p'_{SS} space. It is also an objective measure of scatter of data points and the validity of representing the data points with a single correlation. It is pertinent to note that (e^*, p'_{SS}) data points described by Yang et al. (2006a) as "one trend line could represent the [data points of the] mixtures" had a RMSD value of 0.043. This value will thus be used as the benchmark.

Yang et al. (2006) studied the influence of including Chengbei non-plastic silt in Hokksund sand, with FC in the range of 0 to 30%. The SS data points as shown in Fig. 4a manifested significant spread as indicated by a half-spread value of 0.147. Furthermore, the SS data points moved downward with increase in FC. These data points were re-plotted in Fig. 4b using e^* in lieu of e (and with "b" calculated using the

proposed equation (5a)). All the 18 data points can be described by a single trend curve as substantiated by a RMSD of 0.026. The data was also analyzed with respect to inter-granular void ratio, e_g, as defined in Eqn (3). The corresponding SS data points as shown in Fig. 4c had a RMSD (measured now in e_g) is 0.073, which evidently is too high for a single correlation to be valid. The data points for FC = 30% fines appear to be a main contribution to the high scatter manifested in Fig. 4c. If only data points for FC in the range of 0 to 20% are used in the calculation, the RMSD based on e_g is reduced to about 0.041, which is still significantly higher than that in terms of e^*. This is consistent with the notion that e_g (defined by Eqn (3)) is an approximation of e^* (defined by Eqn (4)) for low fines content.

Huang et al. (2004) performed a series of laboratory tests on reconstituted sample of Mai Liao Sand (MLS) with silty fines from Central Western Taiwan. The SS source data points, with FC in the range of 0 to 30%, is shown in Fig. 5a. A significant and considerable spread is evident and the corresponding half-spread value of 0.139. These 25 data points plotted in the e^*-p'_{SS} space (Fig. 5b) have a RMSD value of 0.056. Although this value is higher than the benchmark value of 0.043 (based on data described by Yang et al (2006) as represented by a single trend line), it is significantly less than the half-spread. Therefore, a single correlation between e^* (calculated using Eqns (4) and (5a)) and p'_{SS} can only be taken as a first approximation.

Ni et al. (2004) reported the influence of a non-plastic fines on Old Alluvium sand from Singapore. Their SS source data as shown in Fig. 6a had a half-spread of 0.062. However, if these data points were plotted in a e^*-p'_{SS} space as presented in Fig. 6b, these 6 data points followed essentially a single trend, with a small RMSD value of 0.022. It is interesting to note that Ni et al. (2004) selected b = 0.7 for calculating equivalent granular void ratio and also got a single trend line for all the SS data points. The prediction equation (5a) gives b = 0.033 for FC = 9%. This implies that multiple b-values can be obtained by a back-analysis process. Indeed, the fines-in-sand model is not consistent with a high b-value of 0.70 at low fines content and high size ratio.

Zlatovic and Ishihara (1995) reported the influence of fines on Toyoura sand. The fines are milled Toyoura sand and FC is in the range of 0 to 30%. Ni et al. (2004) back analyzed the source data and reported that a single SSL in terms of e^* was achieved by setting $b = 0.25$. As shown in Fig. 7a, the SS source data points, manifested significant and considerable spread, as evidenced by a half-spread value of 0.204. If these 37 data points were plotted in the e^*-log(p'_{SS}) space as shown in Fig. 7b, the influence of fines content was significantly reduced as evidenced by a lower RMSD value of 0.048, which is slightly higher than the benchmark value of 0.043 for a single correlation. Furthermore, this scatter was also significantly smaller than that obtained using inter-granular void ratio, e_g, as the alternative state variable as evident from the plot presented in Fig. 7c. These (e_g, p'_{SS}) data points have a RMSD value is 0.075 about the trend curve, which implies the (e_g, p'_{SS}) data points cannot be represented, even approximately, by a single trend curve. It is noted that the threshold fines content was not reported in, and cannot be deduced from, Zlatovic and Ishihara (1995) and an average value of 30% was assigned in the prediction. The sensitivity of the predicted (e*, p'_{SS}) data points to assigned threshold fines content was examined by repeating the prediction with different threshold fines content. No significant reduction of scatter can be achieved by increasing the value of assumed threshold fines content to an upper limit of 35%. However, if the assumed value of threshold fines content was reduced to 25%, (which implies the data points for FC=30% need to be removed from the calculation), the scatter was reduced as shown in Fig. 7d and as evidenced by a smaller RMSD value of 0.035.

Thevanayagam et al. (2002b) presented SS data points for Foundary sand mixed with fines derived from crushed silica, and with FC in the range of 0 to 25%. The source SS data points in the e-p'_{SS} space manifested significant spread (Fig. 8a) as evidenced by a half-spread value of 0.164. These 35 data points when plotted in the e^*-p'_{SS} space (Fig. 8b), could be represented by a single SSL as evidenced by an RMSD value of 0.028.

4.2 Cyclic mobility behaviour

This section investigates whether Cyclic Resistance (CR) as defined in Ishihara (1993) can be correlated to e^* in a manner that is approximately independent of fines content. This evaluation exercise was conducted on four data sets as summarized in Table 1b. It is pertinent to note that the last data set, as explained in a later paragraph, can only be used indirectly. Following the same argument presented for SS data points, the half-spread of the source data based on e and the RMSD of the reduced data points based on e^* were calculated to provide an objective basis for this investigation.

Vaid (1994) performed cyclic triaxial tests on Brenda 20/200 sand with non-plastic fines, and with FC ranges from 0 to 21%. Brenda sand is an angular tailing sand. As shown in Fig. 9a, the Cyclic Resistance versus void ratio relationship is dependent on FC, and the trend lines moves downward with increase in FC. These 13 source data points have a half-spread of 0.165. However, if these data points were re-plotted based on e^* (Fig. 9b), an essentially single correlation between e^* and CR, with a low RMSD of 0.016, was obtained.

Polito (1999) preformed cyclic triaxial tests on Yatesville sand with Yatesville fines. Yatesville sand is a poorly graded, medium to fine sand obtained from a dam site in Louisa County, Kentucky. The fines was derived from the fine-grained portion of Yatesville silty sand. As shown in Fig. 10a, the Cyclic Resstance versus void ratio relationship was dependent on fines content, as evidenced by a high half-spread value of 0.128. Furthermore, the trend lines for the source data points moved downward with increase in FC. If these 27 data points were re-plotted using equivalent granular void ratio as the alternative state variable (Fig. 10b), the resultant a RMSD value (with respect to the "best-fit" correlation) was 0.067. Although this RMSD value may be considered as too high for accepting the correlation, its value is still significantly less than the half-spread of the source data. Therefore, the influence of fines content on the correlation with cyclic resistance is significantly reduced, if e^* is used as the alternative state variable.

Polito and Martin (2001) preformed a series of cyclic triaxial tests on Monterey No. 0/30 sand with Yatesville fines. As shown in Fig. 11a, the Cyclic Resistance versus void ratio relationship is dependent on FC, and the trend lines move downward with increase in FC. The half-spread of these source data is 0.152. However, if these 24 data points were re-plotted in terms of e^* as presented in Fig. 11b, a single correlation between e^* and CR was obtained as evidenced by a low RMSD value of 0.027.

Thevanayagam and Martin (2002) studied the effect of fines on liquefaction using Ottawa sand with non-plastic silt. N_L, the number of cycles required to initiate cyclic liquefaction at an imposed cyclic stress ratio of 0.20, were used as a parameter for studying the influence of fines. As such, N_L is only an indirect measure of Cyclic Resistance and this data set can only be used to investigate whether the influence of fines content can be significantly reduced by using e^* in lieu of e. As shown in Fig. 12a, these 30 source data points plotted in the e-N_L space manifested considerable spread and scatter. The half-spread of the source data is 0.144. However, if the data was re-plotted in the e^*-N_L space, the resultant RMSD was 0.054 which showed the influence of FC was significantly reduced via the use of e^*.

4.3 Discussion

A total of nine data sets were examined. Five of which could be described by a single correlation in terms of e^*, as evidenced by RMSD values less than 0.028. The scatter manifested by the remaining data sets deserves further discussion. The SS data set of Zlatovic and Ishihara (1995), when analyzed in term of e^*, gave a RMSD value in the range of 0.035 to 0.048, depending on the assumed threshold fines content. The mid-range value of 0.042 is close to the benchmark value of 0.043 inferred from Yang et al. (2006b). The remaining 2 data sets (Figs. 5 and 12), when analyzed in terms of e^*, had RMSD values of 0.055; and a single correlation in terms of e^* can only be assumed as a first approximation. The last data set (Fig. 10) had a RMSD value of 0.067 in terms of e^*. This value is considered as too high for the use of a single correlation. However, this

RMSD value is still significantly less than the half-spread of the source data, and thus the influence of fines content is significantly reduced if e^* is used as the alternative state variable.

It is important to re-emphasized that Eqn (5a) used to predict b, and thus e^*, contained only one parameter, $m = 2.5$. The correlations can be improved by having the b-values, hence e^*, back-analyzed on a case specific basis, but this is not the objective of the current study. Differentiation of Eqn (4) with respect to "b" also showed that e^* calculated with Eqn (4) is sensitive to the predicted b-value. Therefore, the exercise undertaken in this section provides a stringent evaluation of the proposed concept.

It needs to be re-iterated that Eqn (4) implies that e^* may be approximated by e_g (calculated with b=0) at low fines content and therefore the importance of predicting a b-value (by Eqn (5a)) is only significant at higher fines content. However, having a unified framework for the whole spectrum of fines content that satisfy the fines-in-sand model is an essential objective of this paper, in particular in relation to the application of Critical State Soil Mechanics framework as presented in the next section.

5 Experimental study by authors

Although the above evaluation was conducted with published data covering a wide range of sand-fines types, the following limitations were identified.

- The fines are non-plastic
- The fines had a relatively low uniformity coefficient: an average value of 4.82 and a maximum value of 7.50
- The published data sets were not established for the objective of evaluating Eqns (4) and (5a).

Therefore, an experimental study was conducted with a sand-fines type of which the fines was a well-graded low plasticity fines. It consists of 2/3 being a natural well-graded silt referred to as Majura Silt (Lo and Wardani 2002; Lo et al. 2003) and 1/3 being Kaolin. It is of low plasticity and has a uniformity coefficient of 12.56. The host sand is a quartz

sand referred to as Sydney sand and its properties were reported in Chu et al. (1992). Fines content in the range of 0 to 30 % were studied. The grading curves of the resultant sand-fines mixtures are presented in Fig. 13.

It is recognized that the identification of SS in an undrained test can be adversely affected by non-uniformity of specimen deformation. Therefore, special experimental techniques including the use of 100mm diameter by 100mm height specimen with free-ends (Bobei and Lo 2001; Lo et al. 1989) were employed. The deformation of the specimen remained essentially uniform even when the axial strain of the specimen exceeded 30% strain (Bobei and Lo 2001). Thus the SS parameters could be measured with a high degree of confidence.

The applicability of the Critical State Soil Mechanics (CSSM) framework in conjunction with equivalent granular void ratio for prediction of flow and non-flow behaviour was also examined.

5.1 Experimental Methodology

A strain controlled triaxial loading system with fully automated data logging facilities was used for this study. Axial load was measured with an internal load cell. The axial deformation was measured by two independent means: a pair of internal LVDTs mounted directly across the platens and an external LVDT. The former was used in the early stage of shearing whereas the latter was used at large deformation. Cell pressure was controlled by a large capacity Digital Pressure Volume Controllers (DPVC). The pore pressure line was connected to a small capacity DPVC for controlling back pressure (and measuring the volume change) at the consolidation stage and for imposing an undrained condition and measuring the resultant pore pressure response. Two pressure transducers were also used to verify pore pressure equilibrium.

A modified moist tamping method was used for specimen preparation to ensure uniformity of the specimen. To accurately control the void ratio and, a total of 10 layers

of predetermined quantities of moist soil were worked into a prescribed thickness. Details of specimen preparation method can be found at Bobei and Lo (2005). Enlarged end platens with free ends, as describe by Lo et al. (1989), was used to minimize end restraint. Liquid rubber technique was used to minimize bedding and membrane penetration error, and also to ensure even seating at the top platen.

Saturation of the specimen was accomplished in two steps; the specimen was initially percolated slowly with carbon dioxide for at least 20 minutes and then back pressure was applied to achieve a B-value of at least 0.98. Filter papers were placed on top and bottom platen porous disk to check fines movement by observing colour and smoothness on the filter paper at the end of the test. It is worth noting that there was no indication of fines movement. The as-formed specimen, measured at a standardized effective confining stress of 20kPa, had a void ratio in the range of 0.927 to 1.019.

5.2 Results and Synthesis

The testing program covering a total of 23 isotropically consolidated undrained (ICU) triaxial tests are summarized in Table 2. Another six ICU tests on the same sand-fines type with 10% fines were also extracted from Bobei and Lo (2005). The effective consolidation stress was in the range of 100kPa to 1300kPa, and the corresponding void ratio at end of consolidation was in the range of 0.481 to 0.922. A few specimens had lower void ratios (at start of shearing). These tests correspond to specimens being consolidated to high confining stress and with fines content ≥ 20%. The behaviour manifested during undrained shearing was either flow or limited flow.

To verify that SS has been attained, both the pore pressure and deviator stress are checked to be stationary with shearing, as illustrated in Fig. 14a for test T-08 which manifested “flow” behaviour. Specimen manifesting “limited flow” were also sheared to Steady States as illustrated by Fig. 14b, with the exception of four tests as marked (‡) in Table 2. This was because the experimental techniques ensured essentially uniform deformation even at high axial strain (Bobei and Lo 2001). For the four tests which approached but did not clearly reach Steady States at end of shearing, the stress states at

SS were obtained by extrapolation following the procedure of Murthy et al. (2007). These 29 SS data points (as plotted in the e-p'_{SS} space) are presented in Fig. 15. As evident from Fig. 15, the SSL in the e-p' space depends on fines content as evidenced by a high half spread value of 0.200, and that the SSL moved downward with increase in fines content. However, when the data is plotted using equivalent granular void ratio in Fig. 16, a single relationship irrespective of fines content, referred hereafter to as Equivalent Granular Steady State Line, is obtained. The corresponding RMSD value in terms of e^* was 0.019. The best-fit equation for the Equivalent Granular Steady State Line is given below:

[6] $$e^*_{ss} = 1 \times 10^{-7} \times \left(p'_{ss}\right)^2 - 0.0003 \times p'_{ss} + 0.9601$$

where e^*_{SS}= equivalent granular void ratio at steady state, p'_{SS} = mean effective stress at steady state. Eqn (6) was used to formulate tests with shearing commencing from a state located slightly above (or below) the equivalent granular SSL in order to provide a stringent verification of the validity of equivalent granular SSL within the CSSM framework.

However, there are some issues on sand with fines that need to be clarified under the CSSM framework. In order to apply the CSSM framework in predicting the undrained behaviour of sand with fines, the SSL specific to the particular fines content needs to be used. This is illustrated by examining two tests T-29 and T-30 with 15% fines. There are sufficient data to define the SSL unambiguously for sand with 15% fines in the e-p' space as illustrated in Fig. 17. Both specimens have essentially the same void ratio at the start of consolidation defined by p' = 25 kPa. Specimen T-29 was sheared from a state located slightly above the SSL for 15% fines, whereas specimen T-30 was sheared from a state located slightly below the SSL for 15% fines. T-29 manifested limited flow whereas T-30 manifested non-flow during undrained shearing. Such a behaviour pattern conforms well to the CSSM framework. The above approach has an obvious limitation, each sand-fines type needs its corresponding SSL and this requires extensive amount of testing. There is an obvious question; can we use the unique

Equivalent Granular SSL to predict the undrained behaviour within the CSSM framework? To answer the above question, the isotropic consolidation and SSL of T-29 and T-30 were re-plotted in Fig. 18 using equivalent granular void ratio as the state variable. T-29 that manifested limited flow had undrained shearing commencing from slightly above the equivalent granular SSL defined by Eqn (6). T-30 which manifested non-flow had undrained shearing commencing from below the equivalent granular SSL. Thus, the undrained behaviour trend of both tests T-29 and T-30 are well predicted using the Equivalent Granular Steady State line in conjunction with CSSM framework. Furthermore, these two tests provide stringent verification of the CSSM framework.

6 Conclusions

This paper examines a simple methodology for predicting equivalent granular void ratio, and thus investigates the use of equivalent granular void ratio as an alternative state variable within the CSSM framework. A simple equation was developed to predict the *b*-value, which was an essential parameter in the calculation of equivalent granular void ratio as defined in Eqn (4). The input parameters for predicting the *b*-value are: size ratio, fines content and threshold fines content. The validity of this prediction methodology was evaluated against 9 published data sets for non-plastic fines. The findings are:

- Out of the five SS data sets examined, the (e^*, p'_{SS}) data points of three data sets can be well represented by a single trend line (or curve) irrespective of fines content. This relationship will be referred to as the "Equivalent Granular Steady State Line". The use of an equivalent granular Steady State Line to describe the other two data sets, however, can only be a first approximation.
- Out of the three data sets for Cyclic Resistance, the (e^*, CR) data points for two data set can be well described by a single trend line/curve. The scatter of the remaining one data set is too high to accept a single relationship, although the influence of fines content on the behaviour pattern is significantly reduced by the use of e^* as the alternative state variable.

- The last data set also showed that the influence of fines content on N_L was significantly reduced if the data was analyzed in term of e^*, despite this data set cannot be used to examine the appropriateness of a single correlation between e* and Cyclic Resistance.

Some of the data sets manifested some scatter from a single relationship. It is recognized that some researchers reported different *b*-values derived by case-specific back-analyses process, and such a process can give less scatter from a single correlation. However, the thrust of this paper is to develop a predictive methodology using simple input parameters. It is somewhat expected that predicted values may not always be as good as back-analyzed values. However, the prediction equation ensures physical reasonableness and can be used as a first approximation for a range of sand-fines types.

Further experimental study was conducted by the authors using a well-graded low plasticity fines. The experimental techniques adopted ensured that SS could reliably attained and the corresponding void ratio could be accurately measured. The findings confirm that the use of Eqn (5a) led to a unique equivalent granular SSL. For the sand-fines type tested by the authors, it was also found that, in undrained shearing, the equivalent granular void ratio, in conjunction with the equivalent granular SSL, may be used to predict the occurrence of flow and the resultant effective stress path. Thus the equivalent granular void ratio may be used as the state variable in lieu of void ratio in the CSSM framework.

The above conclusions are limited to fines that are essentially rotund, which is the inherent assumption in the binary packing study and the nature of fines of the data sets analyzed. When platy fines are involved, the behaviour can be significantly different as reported by Georgiannou (2006).

APPENDIX A

All the source data essentially showed a distinct spread pattern: the SSL or the void ratio versus Cyclic Resistance relationship moved downward with increase in fines content. Therefore the source data is characterized by a half-spread value determined by:

[A1] $$\text{half-spread} = \frac{\int_{X_L}^{X_U} (\overline{e}_1 - \overline{e}_2) dX}{2(X_u - X_L)}$$

where $\overline{e}_1$ is the trend curve (as a function of X) for host sand

$\overline{e}_2$ is the trend curve (as a function of X) for sand with highest fines content

X = p'_{SS} for SS data points

X = Cyclic Resistance (or N_L for Fig. 12) cyclic mobility data points.

Subscript "L" denotes lower-end value of the data range

Subscript "U" denotes upper-end value of the data range

The plots based on *e**, however, have data points clustering or scattering around a trend curve rather that manifesting a clear pattern. Therefore, the root-mean-square deviation (RMSD) as defined below was used:

[A2] $$RMSD = \sqrt{\frac{\sum_i (e_i^* - \hat{e}_i)^2}{N}}$$

Where N is the total number of points in the data set, e_i is the i-th data point and $\hat{e}_i$ is the corresponding void ratio predicted from the best-fit trend line/curve. Three functional forms were used for the best-fit trend curve: linear, quadratic, and power function as proposed by Li et al. (1999); thus giving three RMSD values for each data set. The RMSD value adopted is the lowest value of the three because the corresponding function is the best of the three. It is recognized that this approach will slightly over-estimate the RMSD value as we have not exhaust all possible functional forms.

References

Altun, S., Goktepe, A.B., and Akguner, C. 2005. Cyclic shear strength of silts and sands under cyclic loading. Earthquake Engineering and Soil Dynamics (GSP 133), **158**(40779): 33.

Bobei, D.C., and Lo, S.R. 2001. Static liquefaction of Sydney sand mixed with both plastic and non-plastic Fines. *In* 14th Soughteast Asian Geotechnical Conference. A.A Balkema, Hong Kong. Dec 9-14, pp. 485-491.

Bobei, D.C., and Lo, S.R. 2005. Reverse behaviour and critical state of sand with small amount of fines. *In* The Proceedings of the 16th International Conference on Soil Mechanics and Geotechnical Engineering (16ICSMGE). Japan. Millpress Science Publishers, Rotterdam, Netherlands, Vol.2, pp. 475-478.

Chu, J., and Leong, W.K. 2002. Effect of fines on instability behaviour of loose sand. Géotechnique, **52**(10): 751-755.

Chu, J., Lo, S.R., and Lee, I.K. 1992. Strain softening of granular soil in strain path testing. Journal of Geotechnical Engineering, ASCE, **118**(2): 191-208.

Georgiannou, V.N. 2006. The undrained response of sands with additions of particles of various shapes and sizes. Géotechnique, **56**(9): 639-649.

Georgiannou, V.N., Burland, J.B., and Hight, D.W. 1990. The undrained behaviour of clayey sands in triaxial compression and extension. Géotechnique, **40**(3): 431-449.

Georgiannou, V.N., Hight, D.W., and Burland, J.B. 1991. Undrained behaviour of natural and model clayey sands. Soils and Foundations, **31**(3): 17-29.

Hight, D.W., and Georgiannou, V.N. 1995. Effects of sampling on the undrained behaviour of clayey sands. Géotechnique, **45**(2): 237-247.

Huang, Y.-T., Huang, A.-B., Kuo, Y.-C., and Tsai, M.-D. 2004. A laboratory study on the undrained strength of silty sand from Central Western Taiwan. Soil Dynamics and Earthquake Engineering, **24**: 733-743.

Ishihara, K. 1993. Liquefaction and flow failure during earthquakes. Géotechnique, **43**(3): 351-415.

Kenney, T.C. 1977. Residual strength of mineral mixture. *In* Proc. 9th International Conference of Soil Mechanics and Foundation Engineering, Vol.1, pp. 155-160.

Kuerbis, R., Negussey, D., and Vaid, Y.P. 1988. Effect of gradation and fine content on the undrained response of sand. *In* Hydraulic fill structure, Geotechnical Special Publication 21, ASCE. *Edited by* D.J.A.V. Zul and S.G. Vick. New York, pp. 330-345.

Lade, P.V., Liggio, C.D., and Yamamuro, J.A. 1998. Effects of non-plastic fines on minimum and maximum void ratios of sand. Geotechnical Testing Journal, **21**(4): 336-347.

Li, X.-S., Defalias, Y.F., and Wang, Z.-L. 1999. State-dependent dilatancy in critical-state constitutive modelling of sand. Canadian Geotechnical Journal, **36**(4): 599.

Lo, S.R., and Wardani, S.P.R. 2002. Strength and dilatancy of a silt stabilized by cement and fly ash mixture. Canadian Geotechnical Journal, **39**(1): 77.

Lo, S.R., Chu, J., and Lee, I.K. 1989. A Technique for reducing membrane penetration and bedding errors. Geotechnical Testing Journal, **12**(4): 311-316.

Lo, S.R., Lade, P.V., and Wardani, S.P.R. 2003. An experimental study of the mechanics of two weakly cemented soils. Geotechnical Testing Journal, **26**(3): 328-341.

McGeary, R.K. 1961. Mechanical packing of spherical particles. Journal of the American Ceramic Society, **44**(10): 513-522.

Mitchell, J.K. 1976. Fundamental of soil behaviour. John Wiley & Sons, Inc.

Murthy, T.G., Loukidis, D., Carraro, J.A.H., Prezzi, M., and Salgado, R. 2007. Undrained Monotonic Response of Clean and Silty Sands. Géotechnique, **57**(3): 273-288.

Ni, Q., Dasari, G.R., and Tan, T.S. 2006. Equivalent granular void ratio for characterization of Singapore's Old Alluvium. Canadian Geotechnical Journal, **43**: 563-573.

Ni, Q., Tan, T.S., Dasari, G.R., and Hight, D.W. 2004. Contribution of fines to the compressive strength of mixed soils. Géotechnique, **54**(9): 561-569.

Ni, Q., Tan, T.S., Dasari, G.R., and Hight, D.W. 2005. Discussion: Contribution of fines to the compressive strength of mixed soils. Géotechnique, **55**(8): 627-628.

Ovando-Shelley, E., and Pérez, B.E. 1997. Undrained behaviour of clayey sands in load controlled triaxial tests. Géotechnique, **47**(1): 97-111.

Polito, C.P. 1999. The effects of non-plastic and plastic fines on the liquefaction of sandy soils. PhD thesis in Civil Engineering, The Virginia Polytechnic Institute and State University, Blacksburg, USA.

Polito, C.P., and Martin, J.R. 2001. Effects of nonplastic fines on the liquefaction resistance of solids. Journal of Geotechnical and Geoenvironmental Engineering, **127**(5): 408-415.

Thevanayagam, S. 1998. Effect of fines and confining stress on undrained shear strength of silty sands. Journal of Geotechnical and Geoenvironmental Engineering, **124**(6): 479-491.

Thevanayagam, S. 2000. Liquefaction potential and undrained fragility of silty soils. *In* Proc. 12th World Conf. Earthquake Engineering. *Edited by* R. Park. Auckland, New Zealand. New Zealand Society of Earthquake Engineering, p. Paper #2383.

Thevanayagam, S. 2001. Role of intergranular contacts on the mechanisms causing liquefaction and slope failures in silty sands. *In* Annual project summary report, USGS Award Number: 01HQGR0032. US Geological Survey, Department of Interior, USA.

Thevanayagam, S., and Martin, G.R. 2002. Liquefaction in silty soils-screening and remediation issues. Soil Dynamics and Earthquake Engineering, **22**(9-12): 1035-1042.

Thevanayagam, S., Kanagalingam, T., and Shenthan, T. 2002a. Contact density-Confining Stress-Energy to liquefaction. *In* 15th ASCE Engineering Mechanics Conference. Columbia University, New York.

Thevanayagam, S., Shenthan, T., Mohan, S., and Liang, J. 2002b. Undrained fragility of clean sands, silty sands, and sandy silts. Journal of Geotechnical and Geoenvironmental Engineering, **128**(10): 849-859.

Troncoso, J.H., and Verdugo, R. 1985. Silt content and dynamic behaviour of tailing sands. *In* Proc. 11th International Conference on Soil Mechanics and Foundation Engineering, Vol.3, pp. 1311-1314.

Vaid, Y.P. 1994. Liquefaction of silty soils in Ground Failure under Seismic Conditions. Geotech. Spl. publ. No. 44, S. Prakash and P. Dakoulas (eds.): 1-16.

Wickland, B.E., Wilson, G.W., Wijewickreme, D., and Klein, B. 2006. Design and evaluation of mixtures of mine waste rock and tailings. Canadian Geotechnical Journal, **43**(9): 928-945.

Xenaki, V.C., and Athanasopoulos, G.A. 2003. Liquefaction resistance of sand–silt mixtures: an experimental investigation of the effect of fines. Soil Dynamics and Earthquake Engineering, **23**: 183-194.

Yang, S.L., Lacasse, S., and Sandven, R.F. 2006. Determination of the transitional fines content of mixtures of sand and non-plastic fines. Geotechnical Testing Journal, **29**(2): 102-107.

Yang, S.L., Sandven, R., and Grande, L. 2006a. Instability of sand-silt mixtures. Soil Dynamics and Earthquake Engineering-11th International Conference on Soil Dynamics and Earthquake Engineering (ICSDEE): Part II, **26**(2-4): 183-190.

Yang, S.L., Sandven, R., and Grande, L. 2006b. Steady-state lines of sand-silt mixtures. Canadian Geotechnical Journal, **43**(11): 1213-1219.

Zlatovic, S., and Ishihara, K. 1995. On the influence of nonplastic fines on residul strength. *In* Proceedings of IS-TOKY0'95/ The First International Conference on Earthquake Geotechnical Engineering/Tokyo/ 14-16 November 1995. *Edited by* K. Ishihara. Tokyo, Japan. A.A. Balkema, Rotterdam, Vol.1, pp. 239-244.

Notations:

e	void ratio
$e_{skeleton}$	Sand skeleton void ratio
e_g	intergranular void ratio
e^*	Equivalent granular void ratio
V_T	total volume of the specimen
G_S	specific gravity of sand
ρ_w	density of water
M	total mass of specimen
M_f	mass of silt in the specimen
b	active fraction of fines in force structure
f_c	fines content in decimal
f_{thre}	threshold fines content in decimal
FC	percentage of fines content (%)
D	large particle diameter
d	small particle diameter
D_{10}	sand particle diameter at 10% finer
D_{50}	sand particle diameter at 50% finer
d_{50}	fines particle diameter at 50% finer
U_c	uniformity coefficient of coarse grain
U_f	uniformity coefficient of fines grain
χ_T	particle size ratio, $\chi_T = D_{50}/d_{50}$
χ	particle size ratio, $\chi = D_{10}/d_{50}$
r	particle size ratio, $r = (1/\chi) = d_{50}/D_{10}$
p'	mean effective stress, $p' = (\sigma_1' + 2\sigma_3')/3$
q	deviatoric stress, $q = (\sigma_1' - \sigma_3')$
p'_{SS}	mean effective stress at steady state
e_{SS}	void ratio at steady state
e^*_{SS}	Equivalent granular void ratio at steady state

Table 1a. Summary of previous research on steady state for sand with fines.

Source	Sand			Fines			Input Parameter			Predicted *b*-value
	Name	D_{10}	U_c	Name	d_{50}	U_f	$r = 1/\chi$	Fines Content (%)	Threshold Fines f_{thre} (%)	
Yang et al. 2006	Hokksund sand	0.225	2.25	Chengbei	0.032	2.32	0.142	0 - 30	30*	0 to 0.335
Huang et al. 2004	Mai Liao sand	0.080	1.75	Mai Liao sand	0.044	2.79	0.550	0 - 30	30*	0 to 0.573
Ni at al. 2004	Old Alluvium	0.209	5.63	Old Alluvium	0.038	5.43	0.182	0 - 09	30†	0 to 0.033
Zlatovic and Ishihara 1995	Toyoura Sand	0.116	1.61	Milled Toyoura sand	0.01	6.08	0.086	0 - 30	30†	0 to 0.314
Thevanayagam et al. 2002b	OS00 #55	0.160	1.69	Sil-co-sil #40	0.010	7.50	0.063	0 - 25	25*	0 to 0.225

* Reported/inferred from literature
† Estimated based on average

Table 1b. Summary of previous research on cyclic resistance for sand with fines.

Source	Sand			Fines			Input parameter			Predicted *b*-value
	Name	D_{10}	U_c	Name	d_{50}	U_f	$r = 1/\chi$	Fines Content (%)	Threshold Fines f_{thre} (%)	
Vaid 1994	Brenda 20/200	0.070	3.92	Non-plastic	0.007	2.97	0.100	0 - 21	30†	0 to 0.171
Polito, P.C. 1999	Yalesville	0.089	2.39	Yatesville silt	0.031	4.38	0.348	0 - 37	37*	0 to 0.534
Polito and Martin 2001	Monterey 0/30	0.311	1.55	Yatesville silt	0.031	4.38	0.100	0 - 25	32*	0 to 0.228
Thevanayagam and Martin 2002	OS00 #55	0.160	1.69	Sil-co-sil #40	0.010	7.50	0.063	0 - 25	25*	0 to 0.226

* Reported/inferred from literature
† Estimated based on average

Table 2. Summary of experimental testing program.

Test No.	Fines Content (%)	At the start of shearing		
		Confining Pressure p' (kPa)	Void ratio, e	Equivalent granular void ratio, e^*
T-21	0	350	0.889	0.889
T-32	0	350	0.780	0.780
T-34	0	600	0.887	0.887
T-36‡	0	600	0.813	0.813
T-35	0	850	0.922	0.922
T-30‡	15	100	0.641	0.889
T-8	15	350	0.693	0.950
T-5	15	600	0.685	0.941
T-26	15	600	0.650	0.900
T-27	15	600	0.654	0.905
T-31‡	15	600	0.558	0.794
T29‡	15	600	0.613	0.857
T-7	15	850	0.684	0.940
T-6	15	1100	0.665	0.918
T-28	15	1300	0.593	0.835
T-22	20	350	0.627	0.942
T-14	20	600	0.632	0.947
T-13	20	850	0.616	0.928
T-25	20	1100	0.627	0.942
T-23	30	350	0.555	0.954
T-9	30	600	0.545	0.941
T-10	30	850	0.486	0.867
T-24	30	1100	0.481	0.861

‡ Approached but did not clearly reach the SS at end of shearing. The stress state at SS was obtained by extrapolation following the procedure of Murthy et al. (2007).

LIST OF FIGURES

Figure 1. Effect of fines content on minimum void ratio of binary mix (After Lade et al. 1998)

Figure 2. Effect of diameter ratio on minimum void ratio of binary mix (After Lade et al. 1998)

Figure 3. Factors affecting *b*; (a) Influence of χ on *b* (TFC=35%), (b) Influence of χ on the first factor of Eqn (5), (c) Influence of fines content on *b* (TFC=35%)

Figure 4. Steady state lines for Hokksund sand with Chengbei non-plastic fines; (a) source data after Yang et al. 2006, (b) interpreted based on *e using Eqn. (4) and (5), (c) interpreted based on e_g using Eqn. (3)**

Figure 5. Steady state lines for Mai Liao sand with fines; (a) source data after Huang et al. 2004, (b) interpreted based on *e using Eqn. (4) and (5)**

Figure 6. Steady state lines for Old Alluvium sand with fines; (a) source data after Ni et al. 2004, (b) interpreted based on *e using Eqn. (4) and (5)**

Figure 7. Steady state lines for Toyoura sand with fines; (a) source data after Zlatovic and Ishihara 1995, (b) interpreted based on *e using Eqn. (4) and (5), (c) interpreted based on e_g using Eqn. (3), (d) interpreted based on *e** using Eqn. (4) and (5) when TFC=25%**

Figure 8. Steady state lines for Foundry sand with non-plastic fines; (a) source data after Thevanayagam et al. 2002, (b) interpreted based on *e using Eqn. (4) and (5)**

Figure 9. Cyclic Resistance for 20/200 Brenda sand with silty fines; (a) source data after Vaid 1994, (b) interpreted based on *e using Eqn. (4) and (5)**

Figure 10. Cyclic resistance for Yatesville sand with fines; (a) source data after Polito 1999, (b) interpreted based on *e using Eqn. (4) and (5)**

Figure 11. Cyclic resistance for Montereysand and Yatesville fines; (a) source data after Polito and Martin 2001, (b) interpreted based on *e using Eqn. (4) and (5)**

Figure 12. No. of cycles (N_L) required to trigger cyclic liquefaction for Ottawa sand with non-plstic fines at cyclic stress ratio of 0.20; (a) source data after Thevanayagam and Martin 2002, (b) interpreted based on *e using Eqn. (4) and (5)**

Figure 13. Grain size distribution curve of Sydney sand and Majura fines with Kaolin

Figure 14. Pore water pressure and deviatoric stress response for (a) flow behaviour (test T-08) and (b) limited flow behaviour (test T-28)

Figure 15. Multiple SSLs for Sydney sand with different fines content

Figure 16. A unique equivalent granular SSL for Sydney sand with different fines content

Figure 17. Consolidation line of tests T-29, T-30 and SSL for Sydney sand with 15% fines

Figure 18. Consolidation line and unique SSL of T-29 and T-30 (Sydney sand with 15% fines)

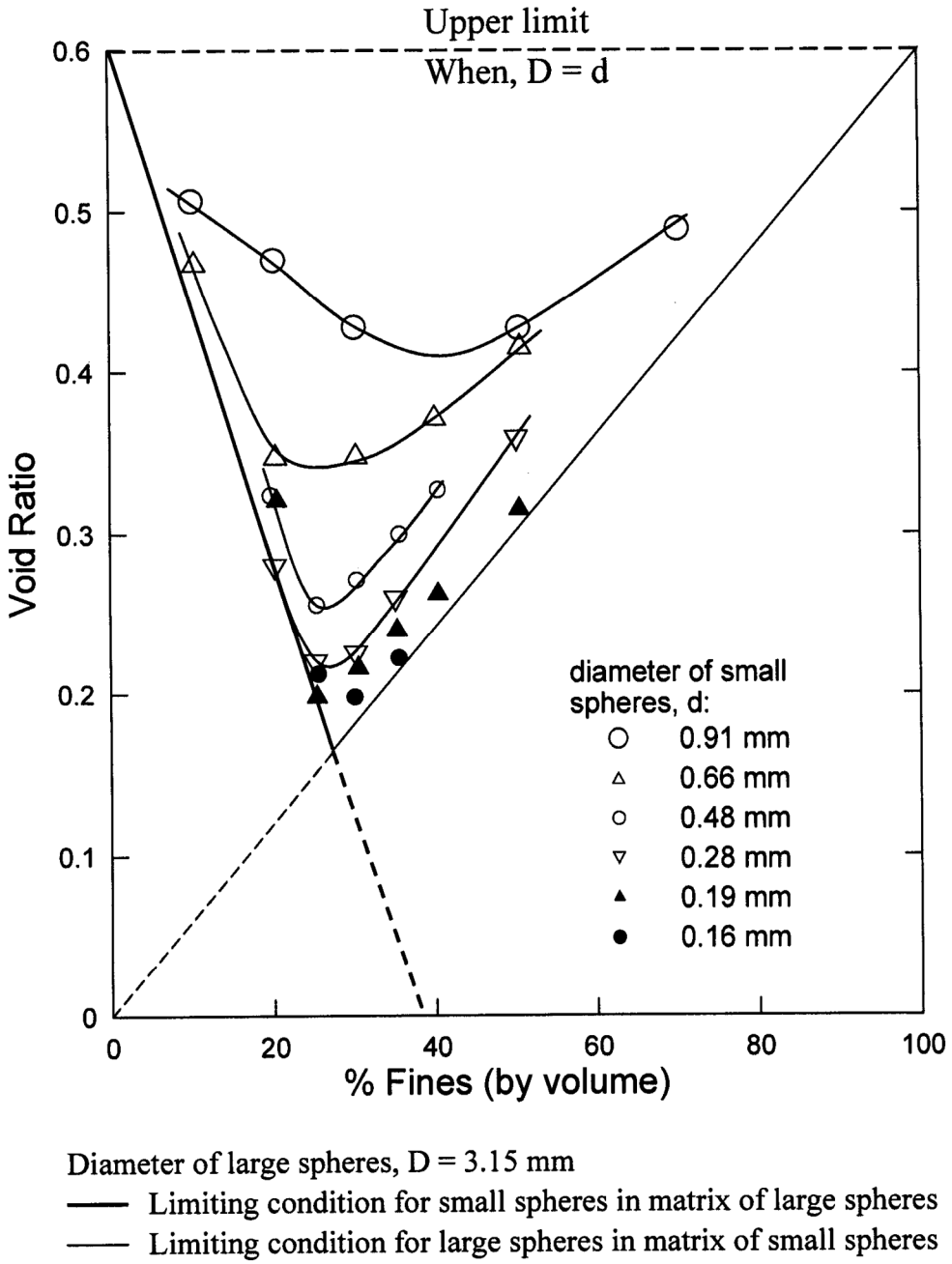

Figure 1. Effect of fines content on minimum void ratio of binary mix (After Lade et al. 1998)

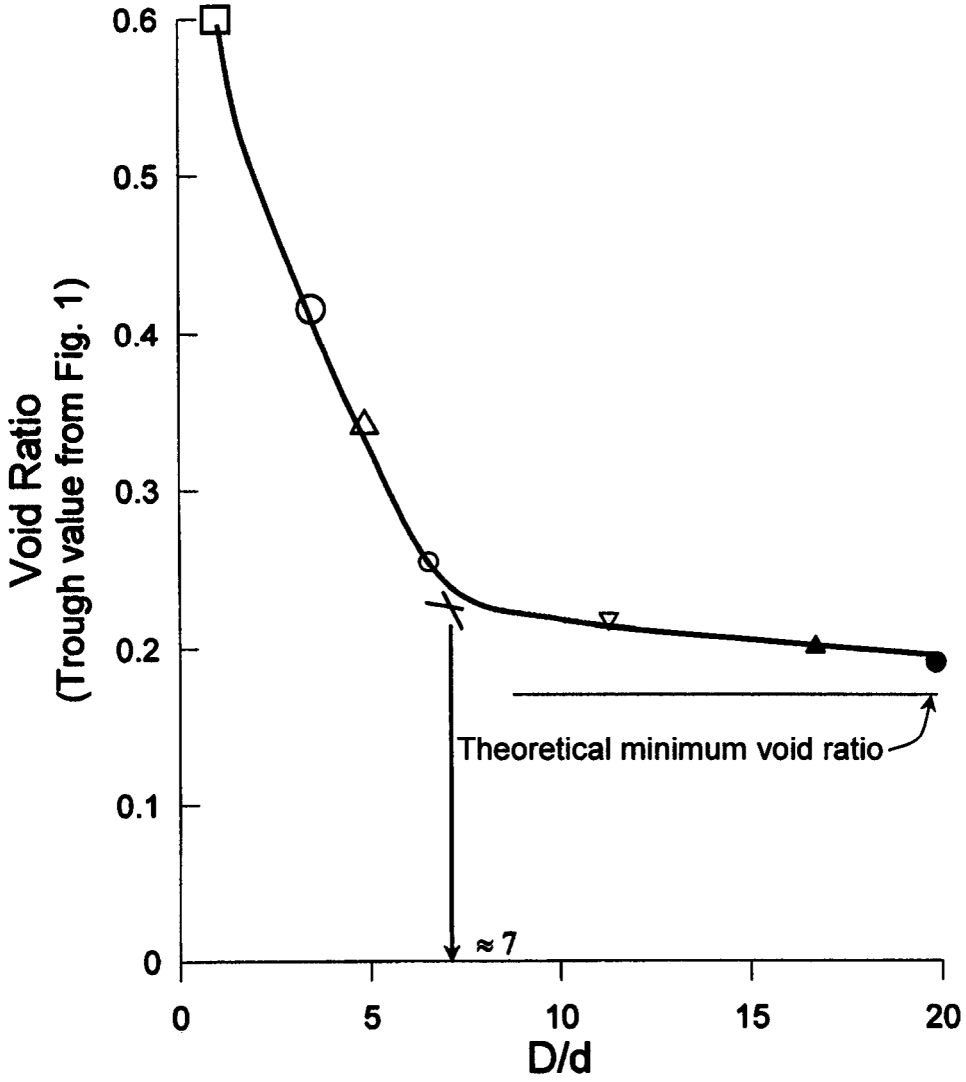

Figure 2. Effect of diameter ratio on minimum void ratio of binary mix (After Lade et al. 1998)

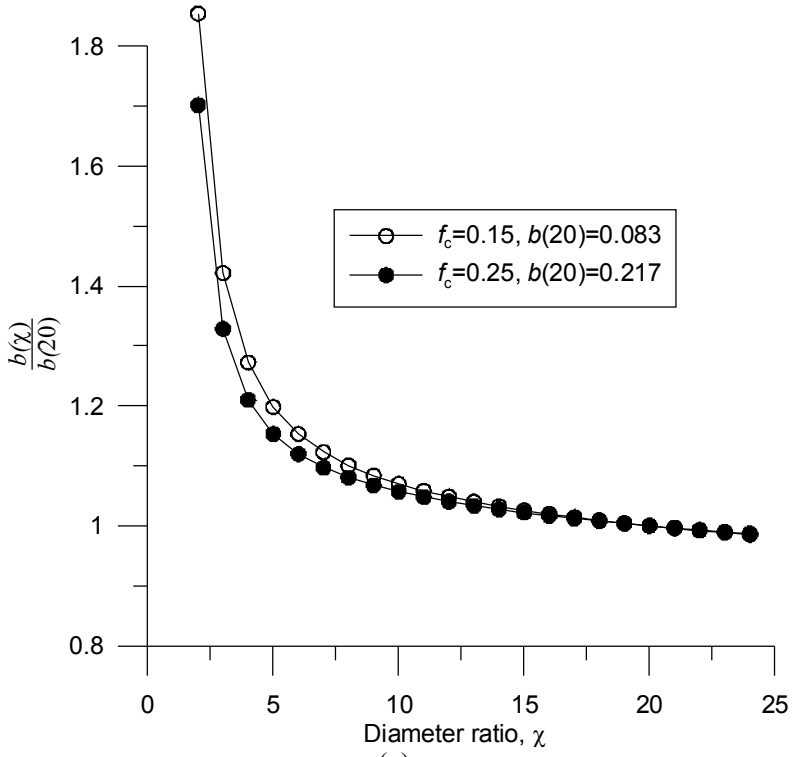

(a)

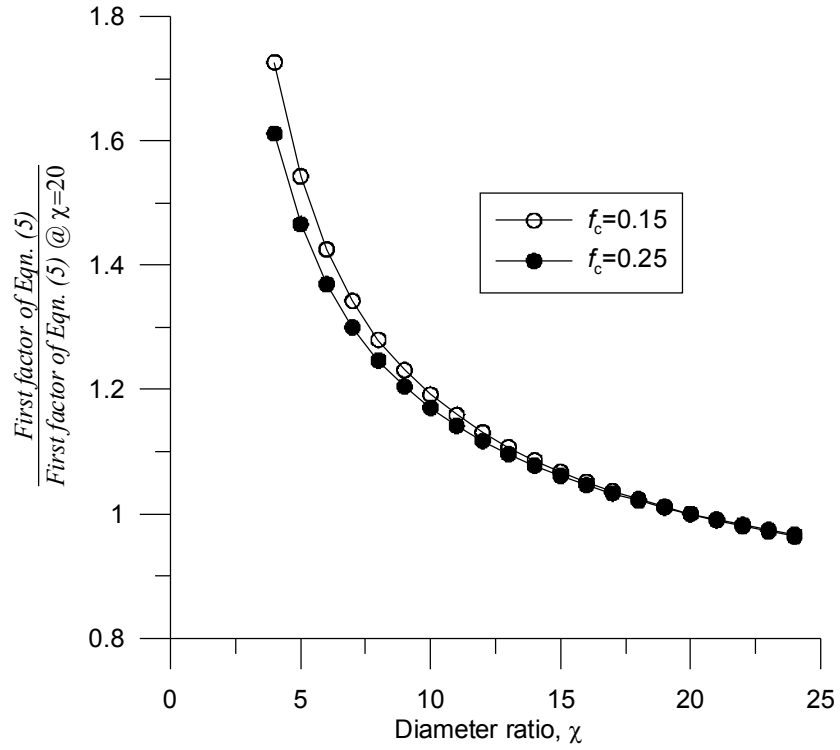

(b)

Figure 3. Factors affecting *b*; (a) Influence of χ on *b* (TFC=35%), (b) Influence of χ on the first factor of Eqn (5), (c) Influence of fines content on *b* (TFC=35%)

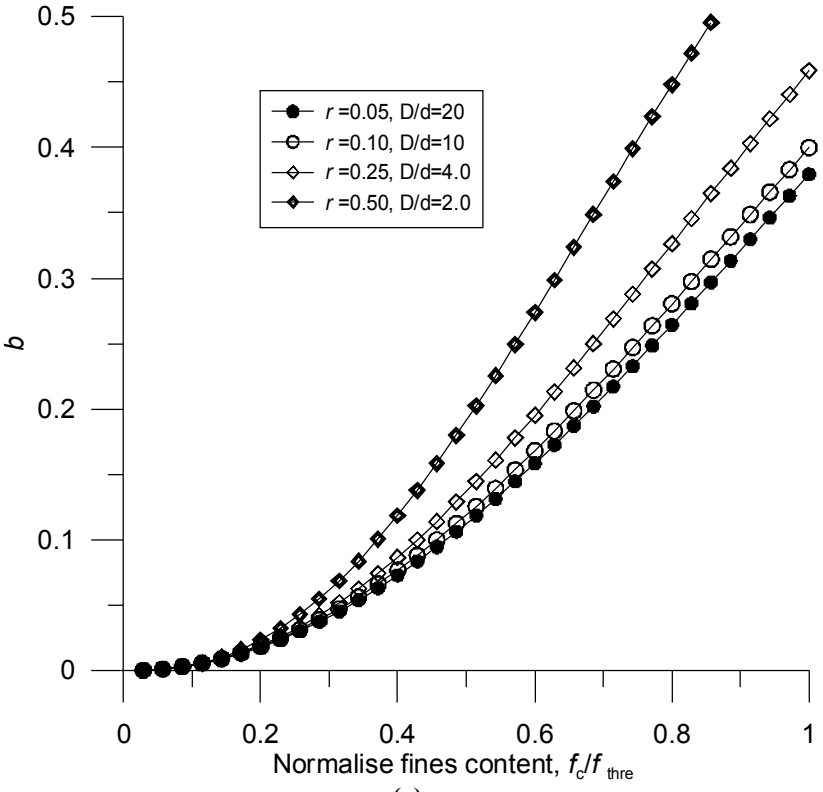

(c)

Figure 3. Factors affecting *b*; (a) Influence of χ on *b* (TFC=35%), (b) Influence of χ on the first factor of Eqn (5), (c) Influence of fines content on *b* (TFC=35%)

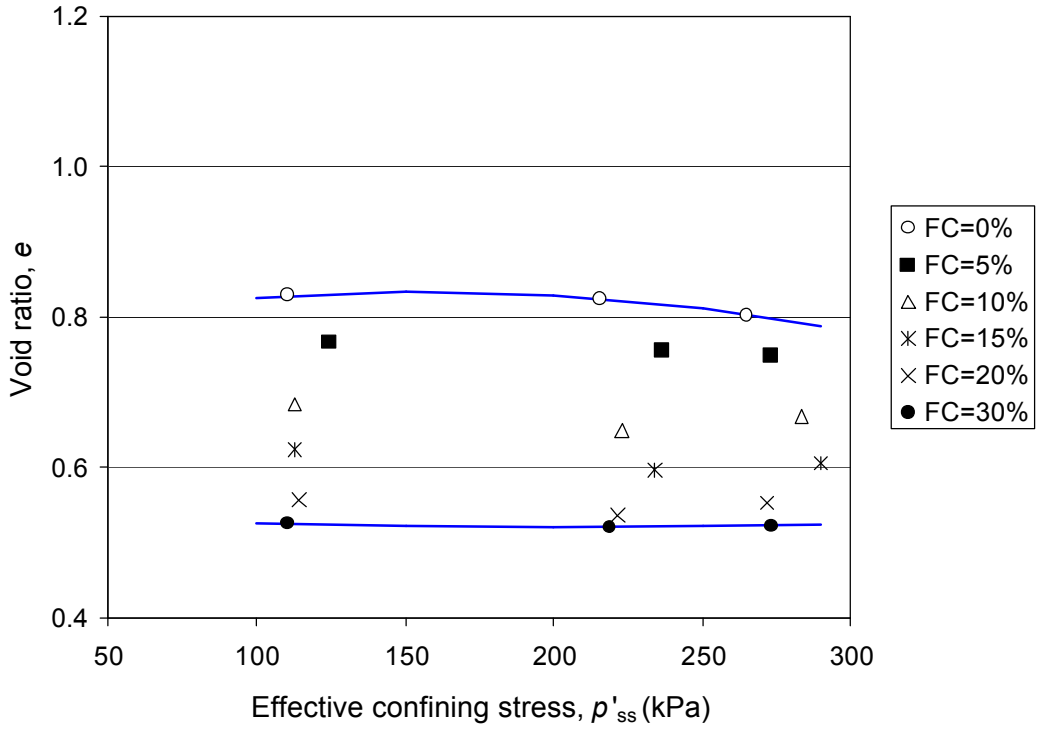

(a)

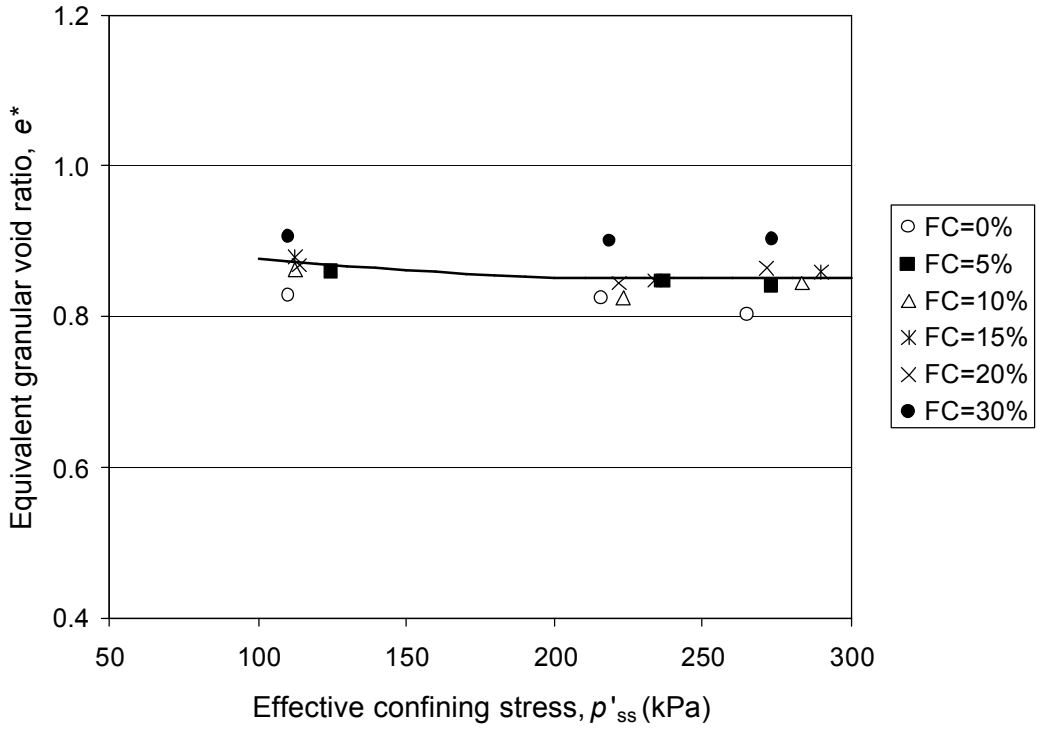

(b)

Figure 4. Steady state lines for Hokksund sand with Chengbei non-plastic fines; (a) source data after Yang et al. 2006, (b) interpreted based on e^* using Eqn. (4) and (5), (c) interpreted based on e_g using Eqn. (3).

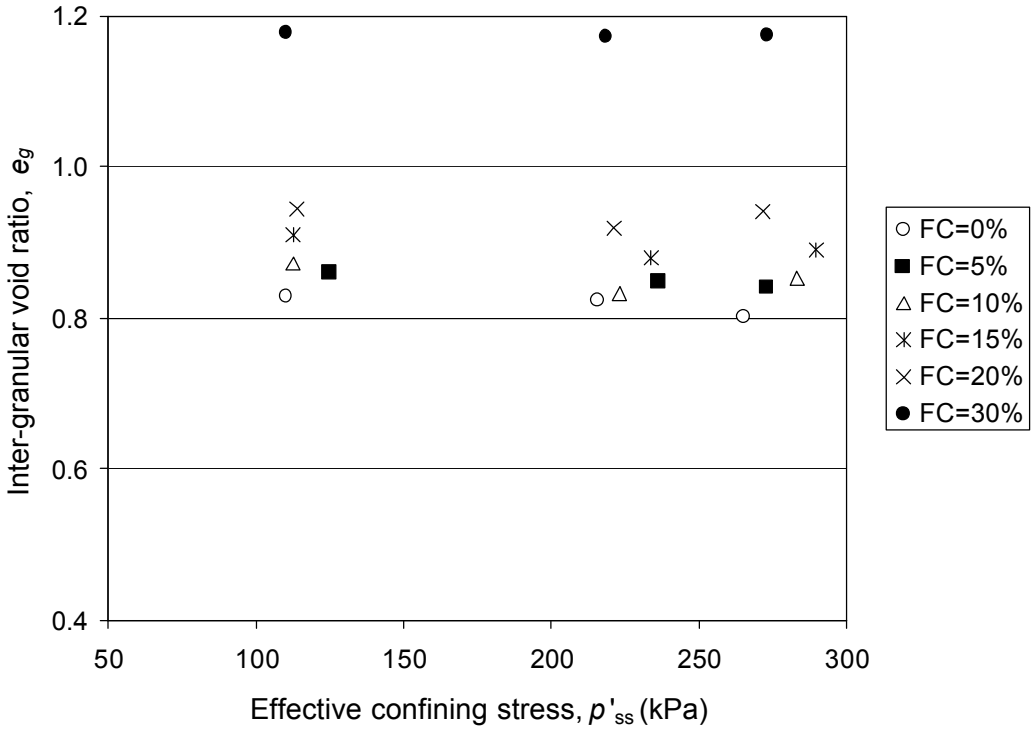

(c)

Figure 4. Steady state lines for Hokksund sand with Chengbei non-plastic fines; (a) source data after Yang et al. 2006, (b) interpreted based on e^* using Eqn. (4) and (5), (c) interpreted based on e_g using Eqn. (3).

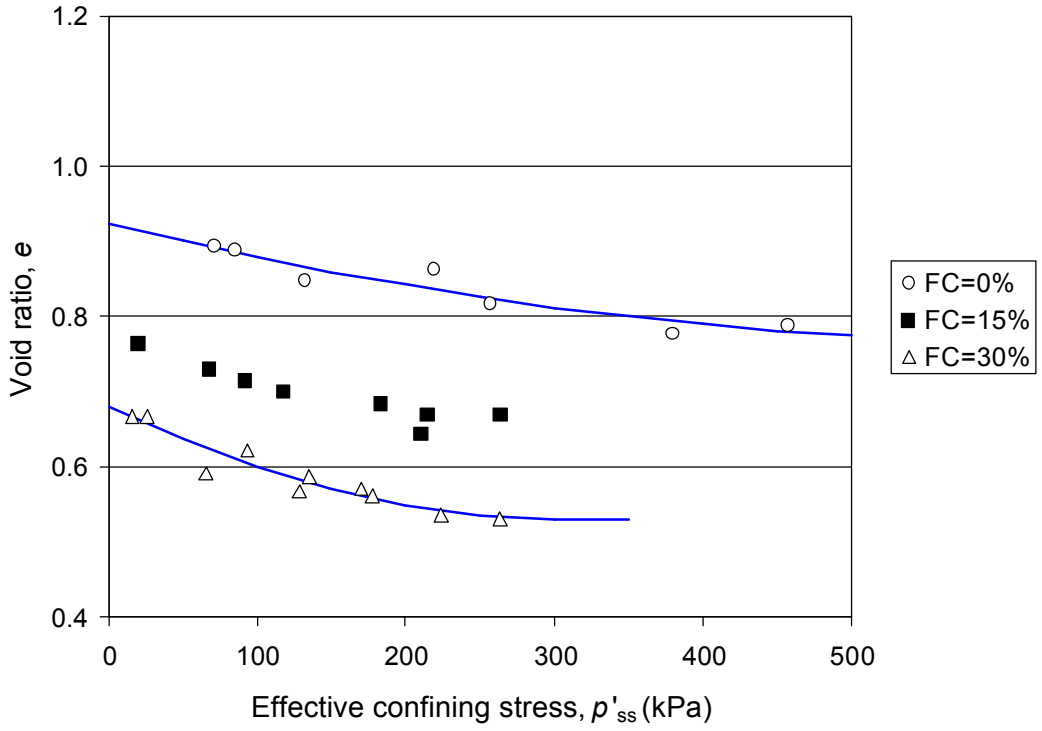

(a)

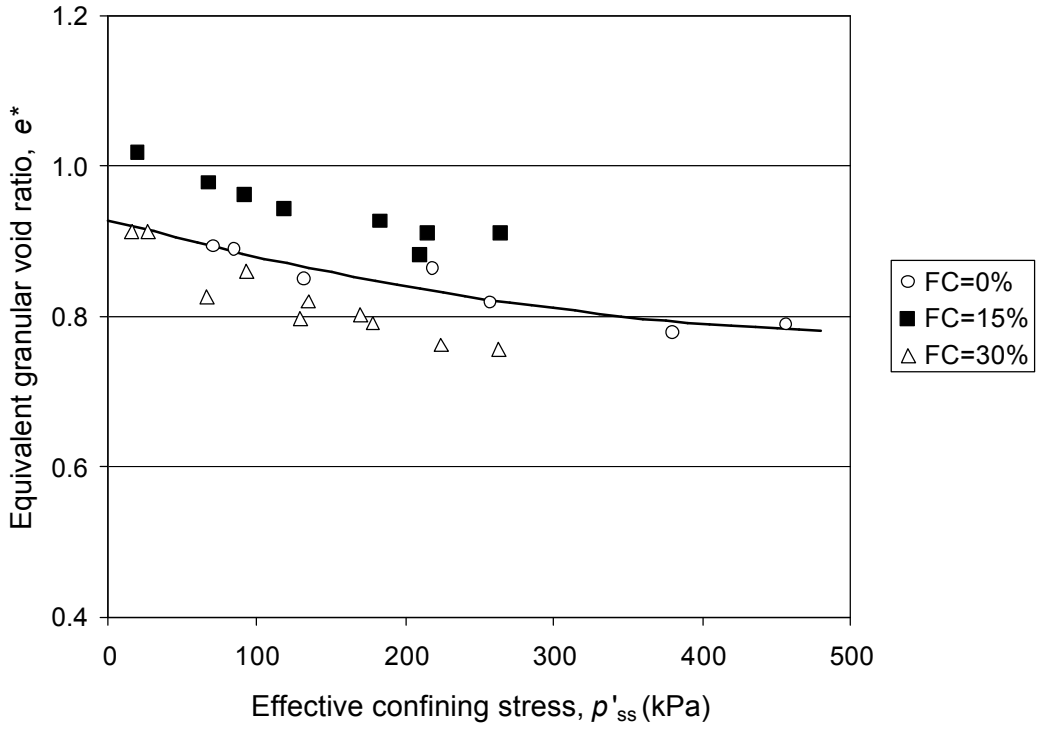

(b)

Figure 5. Steady state lines for Mai Liao sand with fines; (a) source data after Huang et al. 2004, (b) interpreted based on *e using Eqn. (4) and (5)**

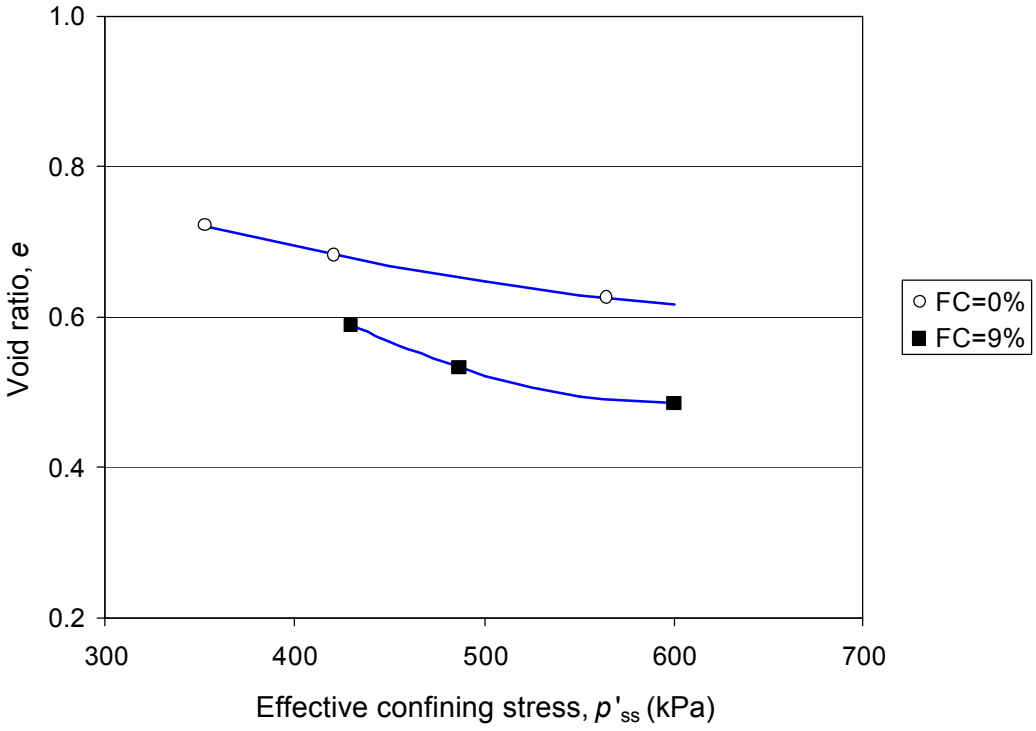

(a)

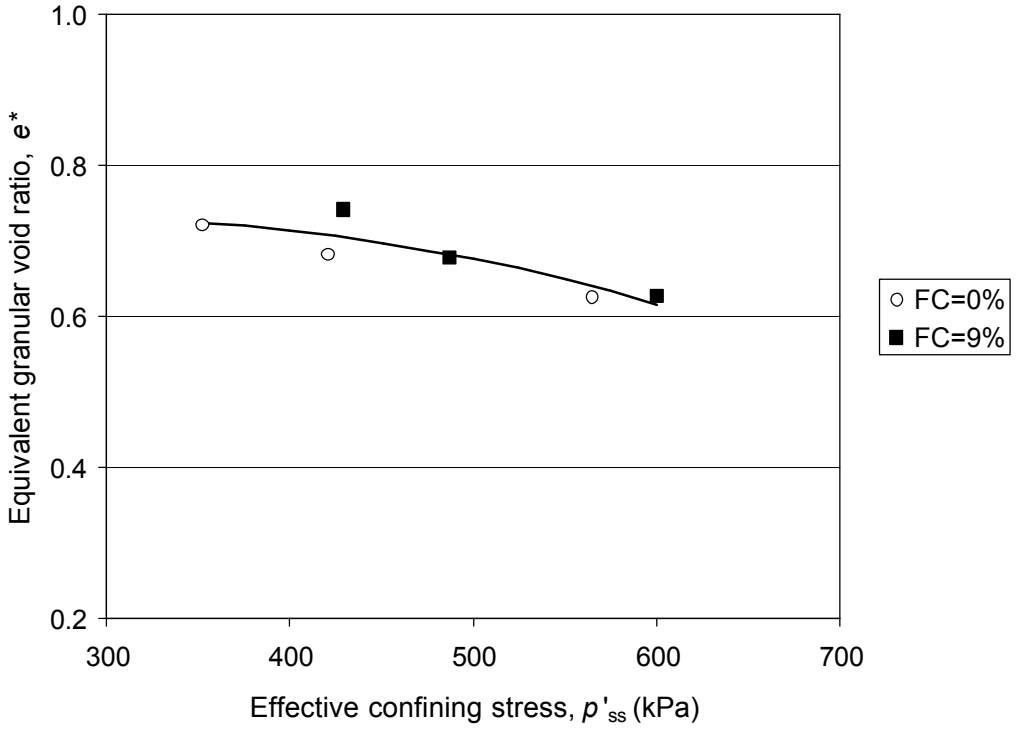

(b)

Figure 6. Steady state lines for Old Alluvium sand with fines; (a) source data after Ni et al. 2004, (b) interpreted based on *e using Eqn. (4) and (5)**

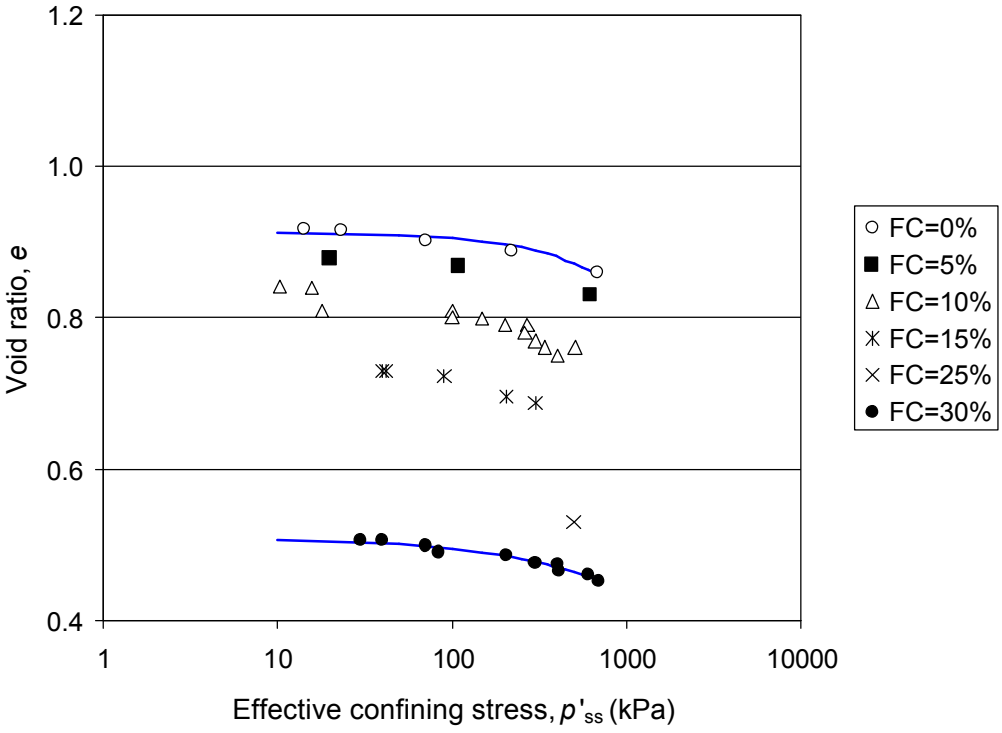

(a)

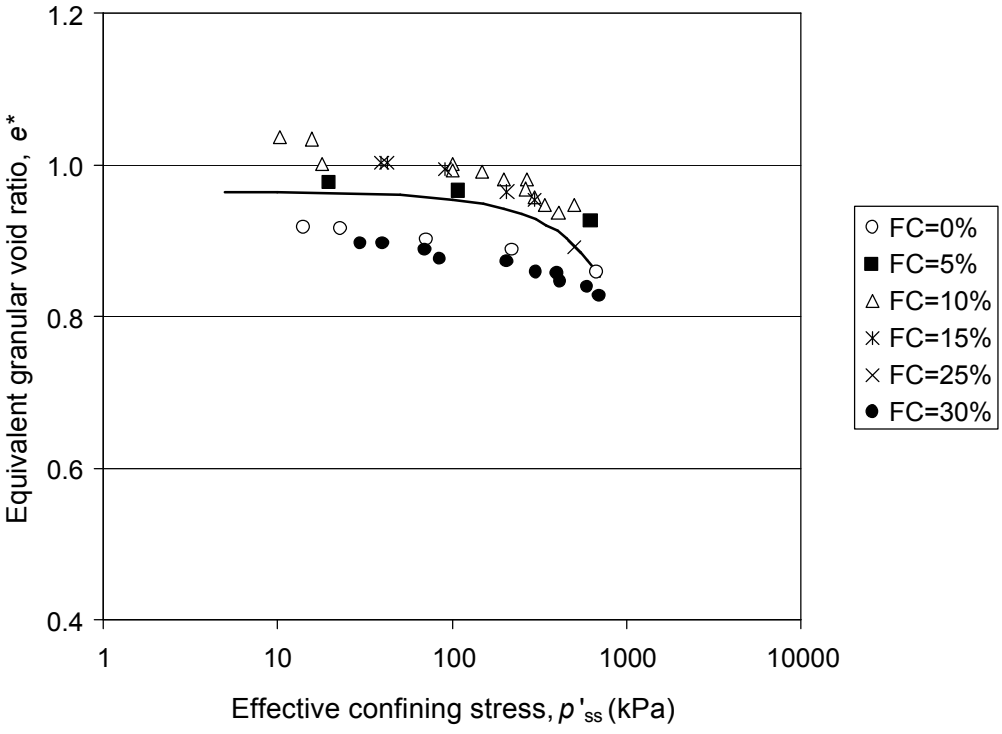

(b)

Figure 7. Steady state lines for Toyoura sand with fines; (a) source data after Zlatovic and Ishihara 1995, (b) interpreted based on *e using Eqn. (4) and (5), (c) interpreted based on e_g using Eqn. (3) (d) interpreted based on *e** using Eqn. (4) and (5) when TFC=25%**

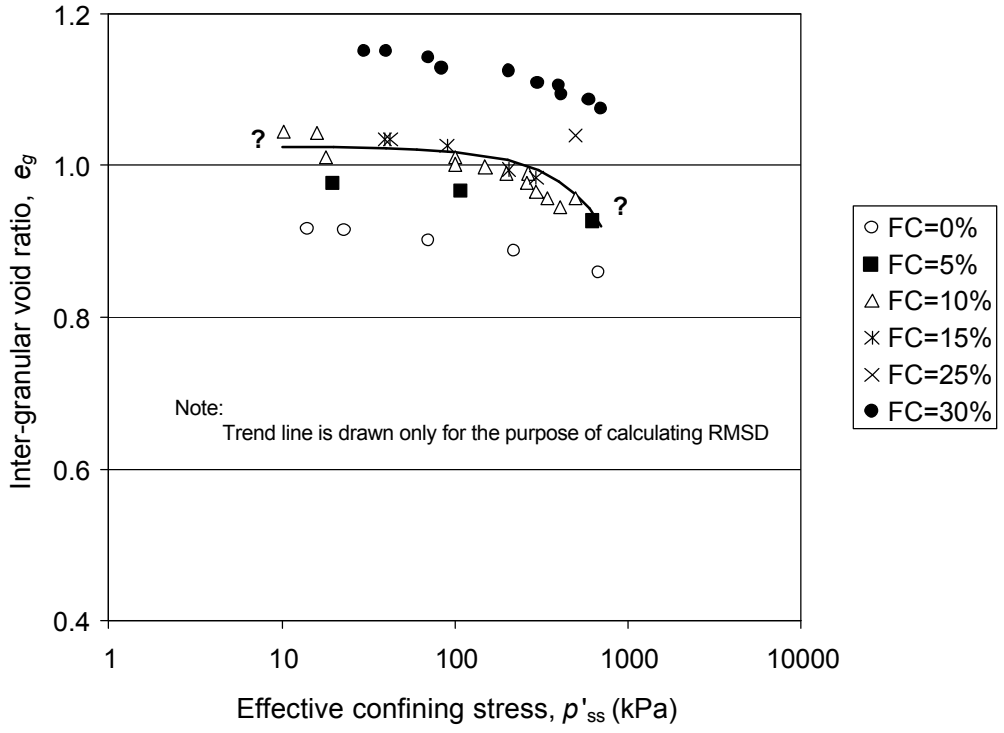

(c)

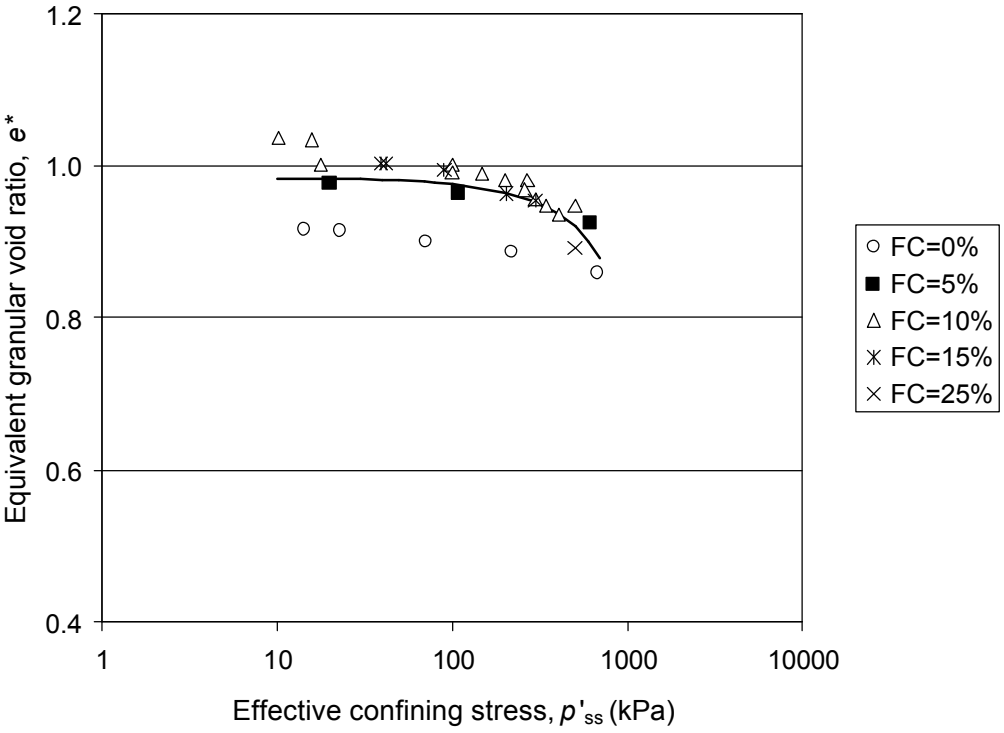

(d)

Figure 7. Steady state lines for Toyoura sand with fines; (a) source data after Zlatovic and Ishihara 1995, (b) interpreted based on e^* using Eqn. (4) and (5), (c) interpreted based on e_g using Eqn. (3) (d) interpreted based on e^* using Eqn. (4) and (5) when TFC=25%

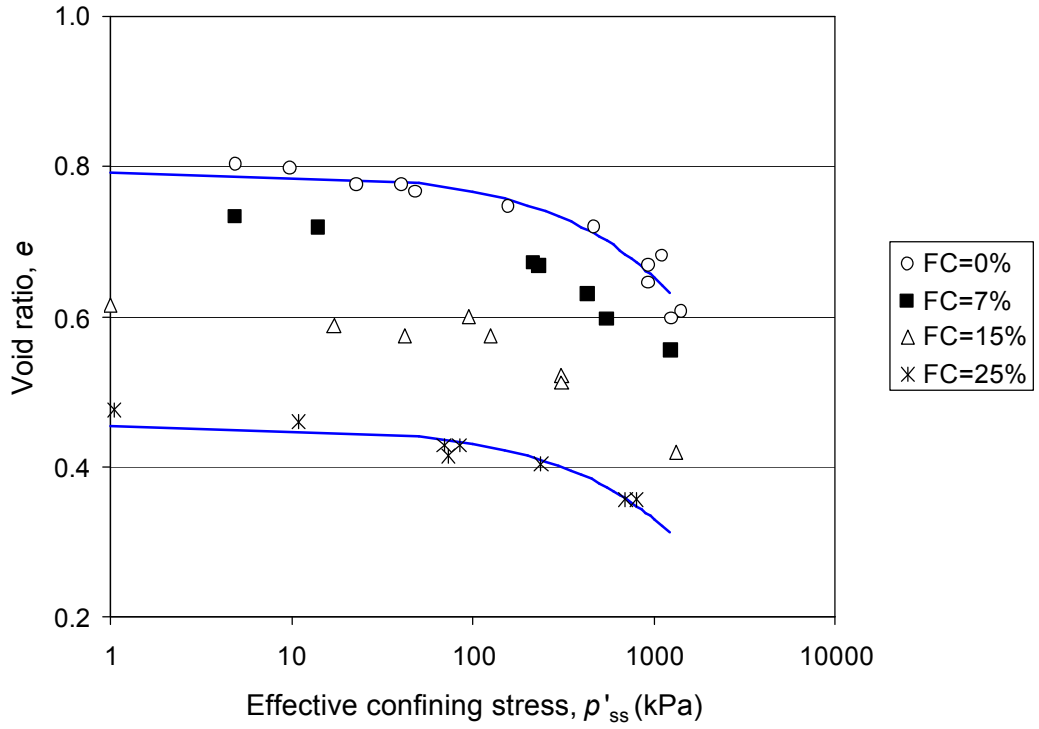

(a)

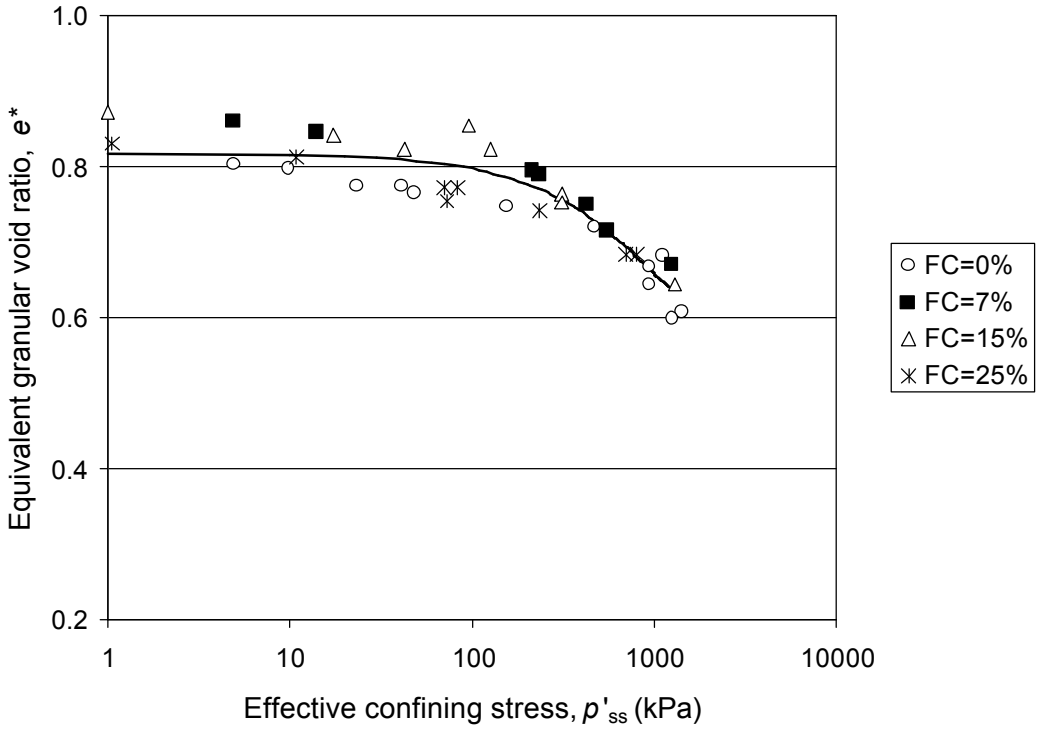

(b)

Figure 8. Steady state lines for Foundry sand with non-plastic fines; (a) source data after Thevanayagam et al. 2002b, (b) interpreted based on *e using Eqn. (4) and (5)**

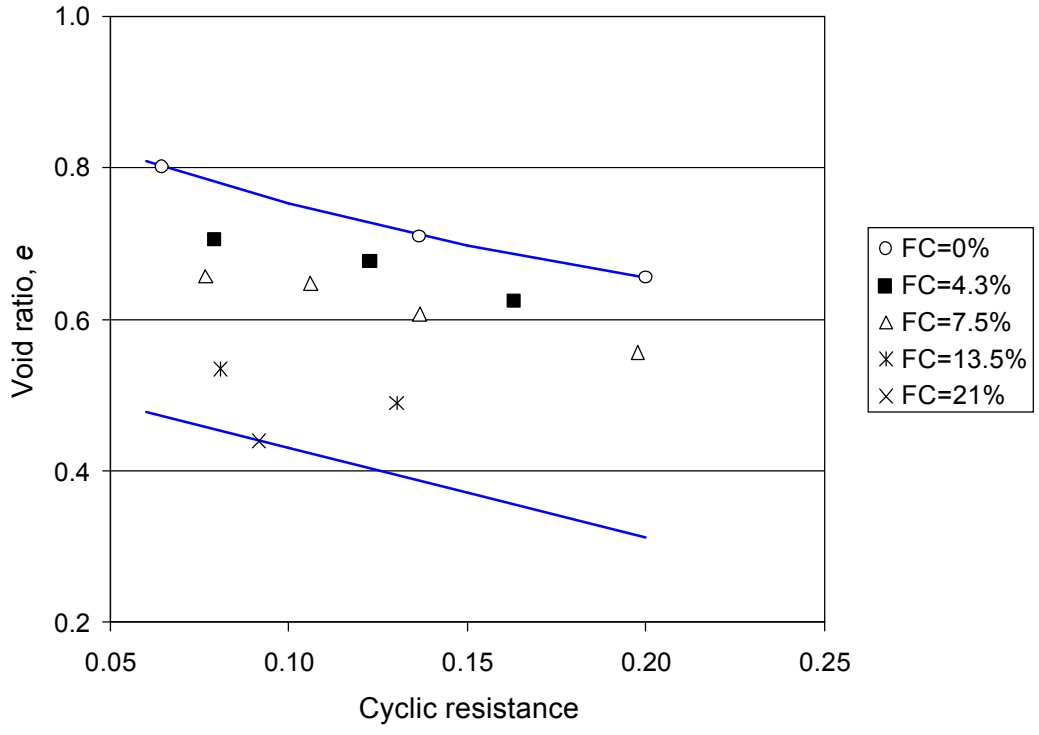

(a)

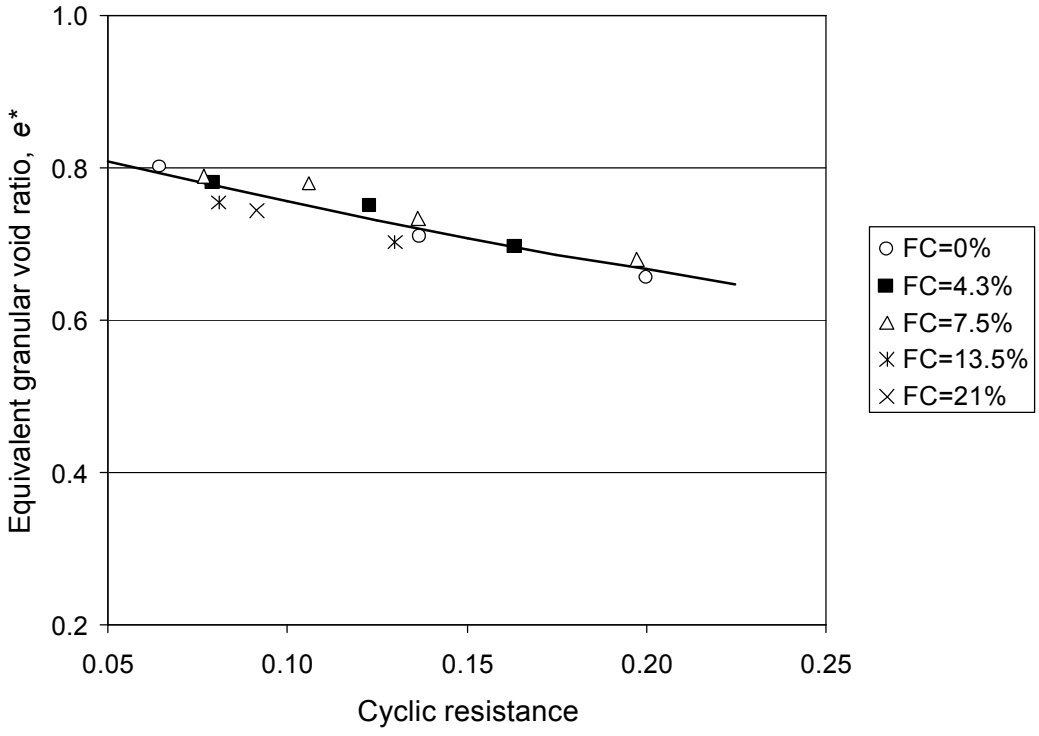

(b)

Figure 9. Cyclic Resistance for 20/200 Brenda sand with silty fines; (a) source data after Vaid 1994, (b) interpreted based on *e using Eqn. (4) and (5)**

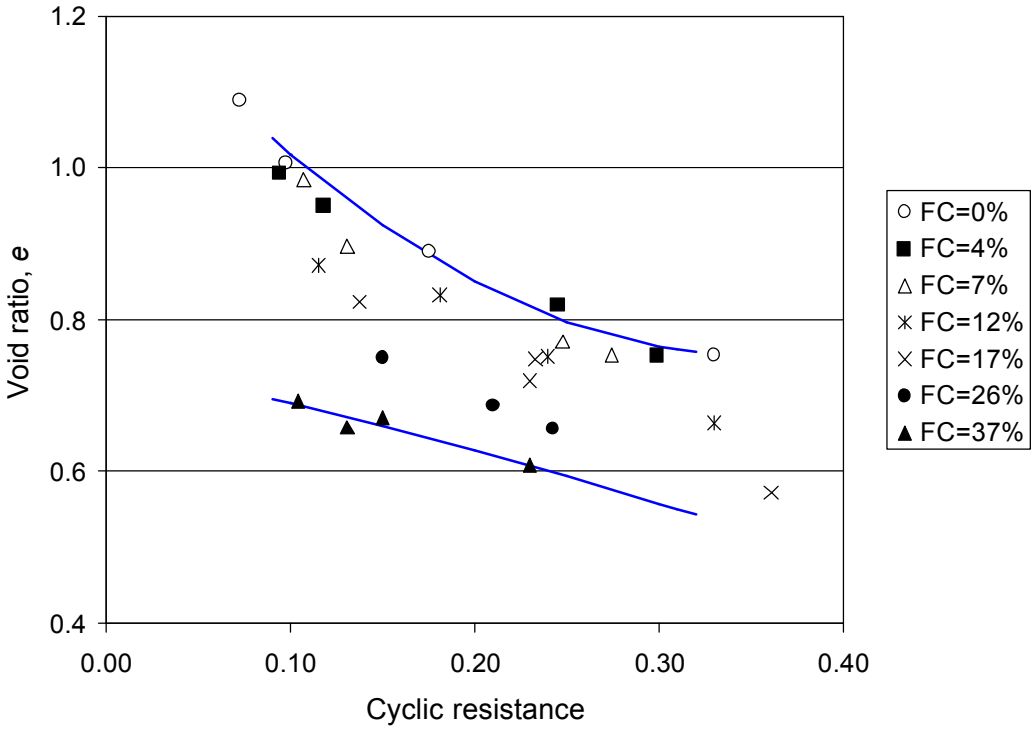

(a)

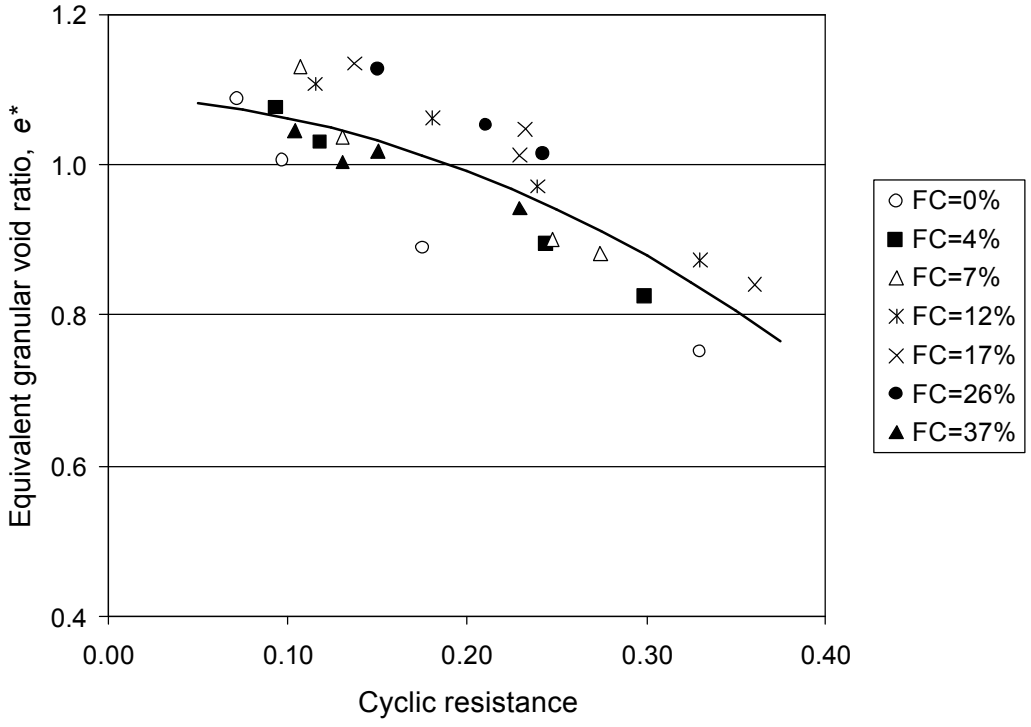

(b)

Figure 10. Cyclic resistance for Yatesville sand with fines; (a) source data after Polito 1999, (b) interpreted based on *e using Eqn. (4) and (5)**

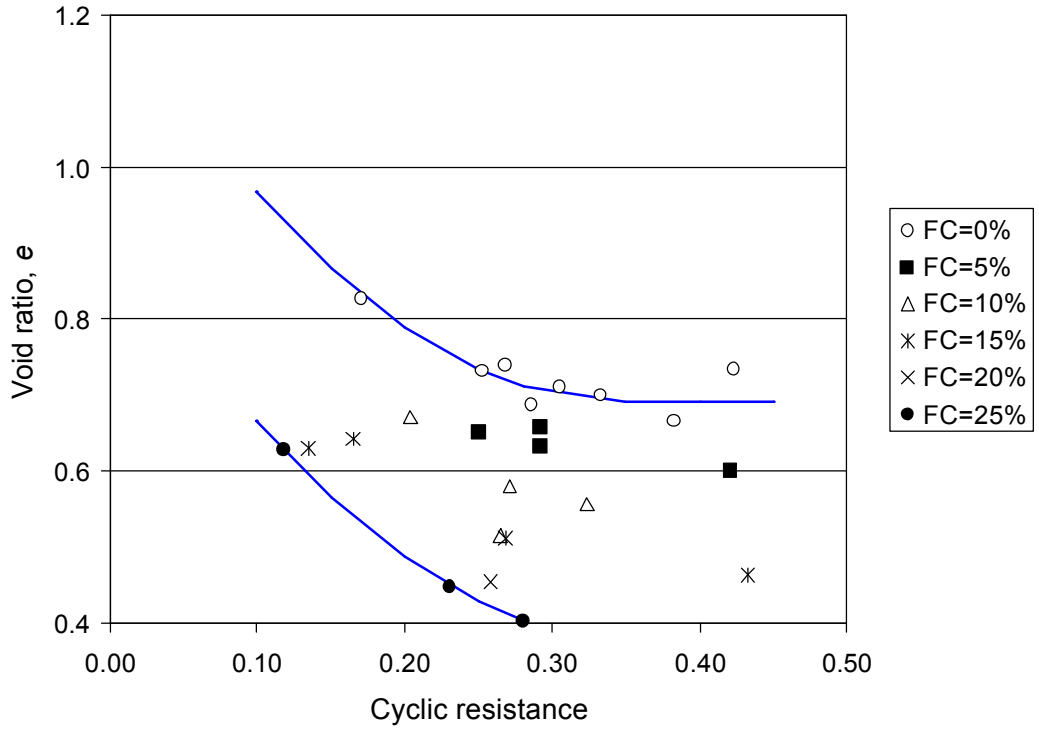

(a)

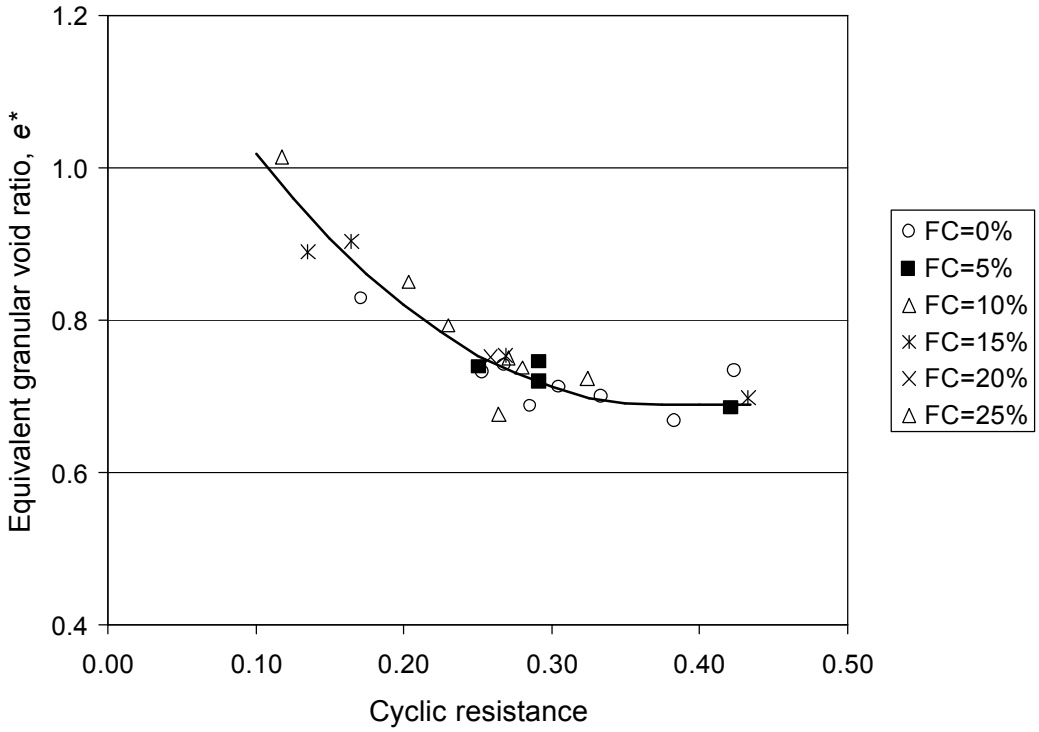

(b)

Figure 11. Cyclic resistance for Monterey sand and Yatesville fines; (a) source data after Polito and Martin 2001, (b) interpreted based on *e using Eqn. (4) and (5)**

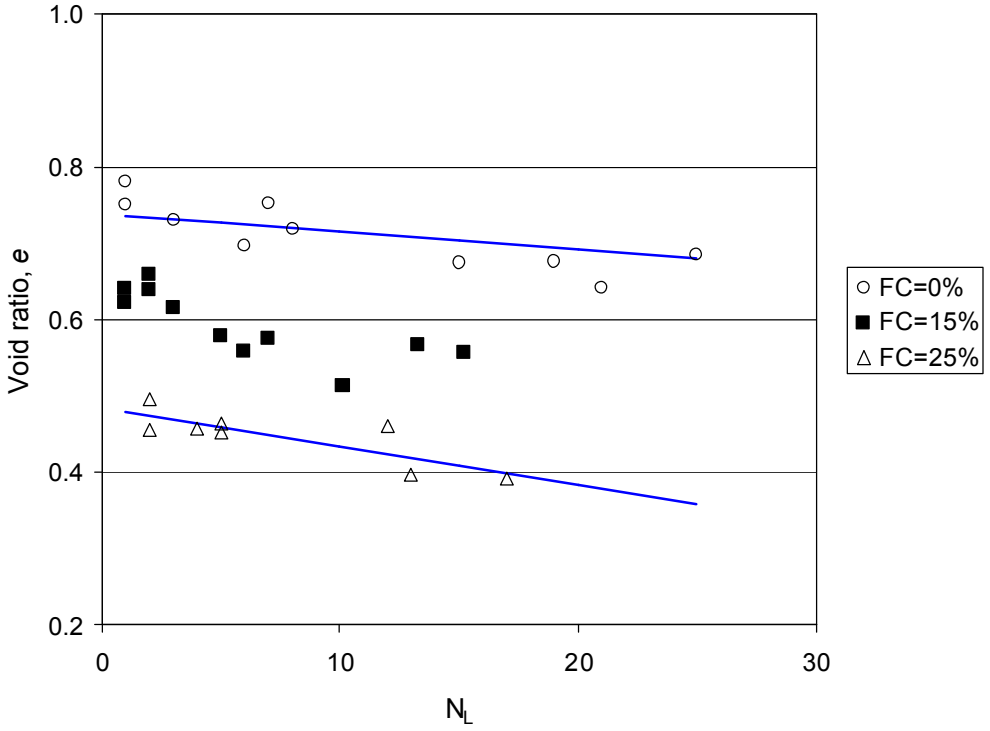

(a)

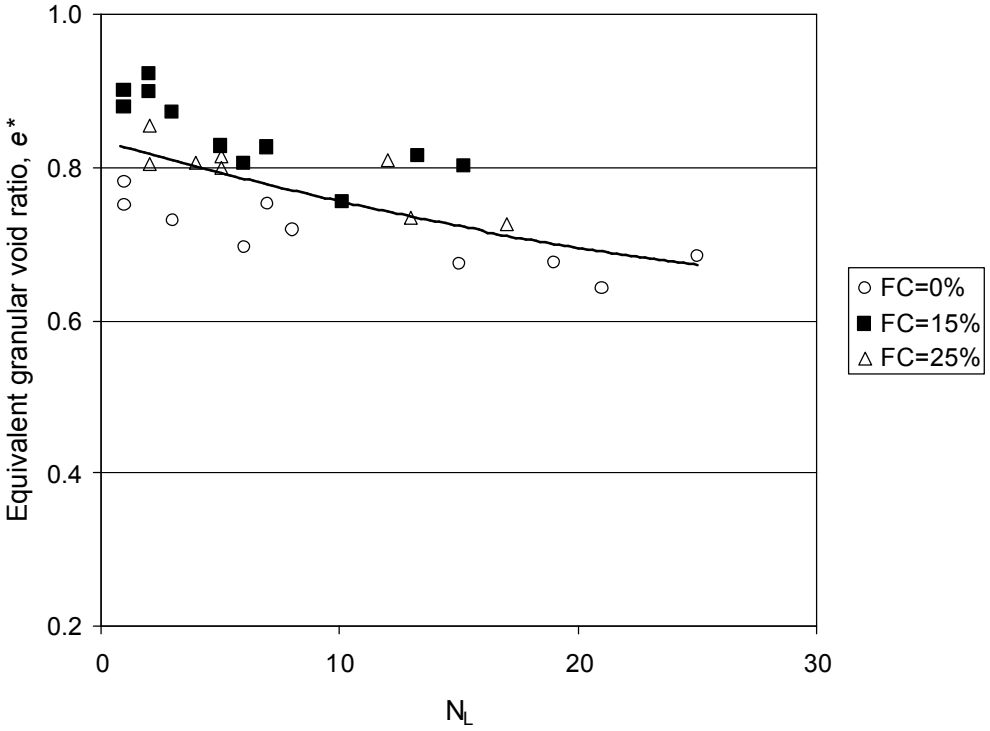

(b)

Figure 12. No. of cycles (N_L) required to trigger cyclic liquefaction for Ottawa sand with non-plastic fines at cyclic stress ratio of 0.20; (a) source data after Thevanayagam and Martin 2002, (b) interpreted based on *e using Eqn. (4) and (5)**

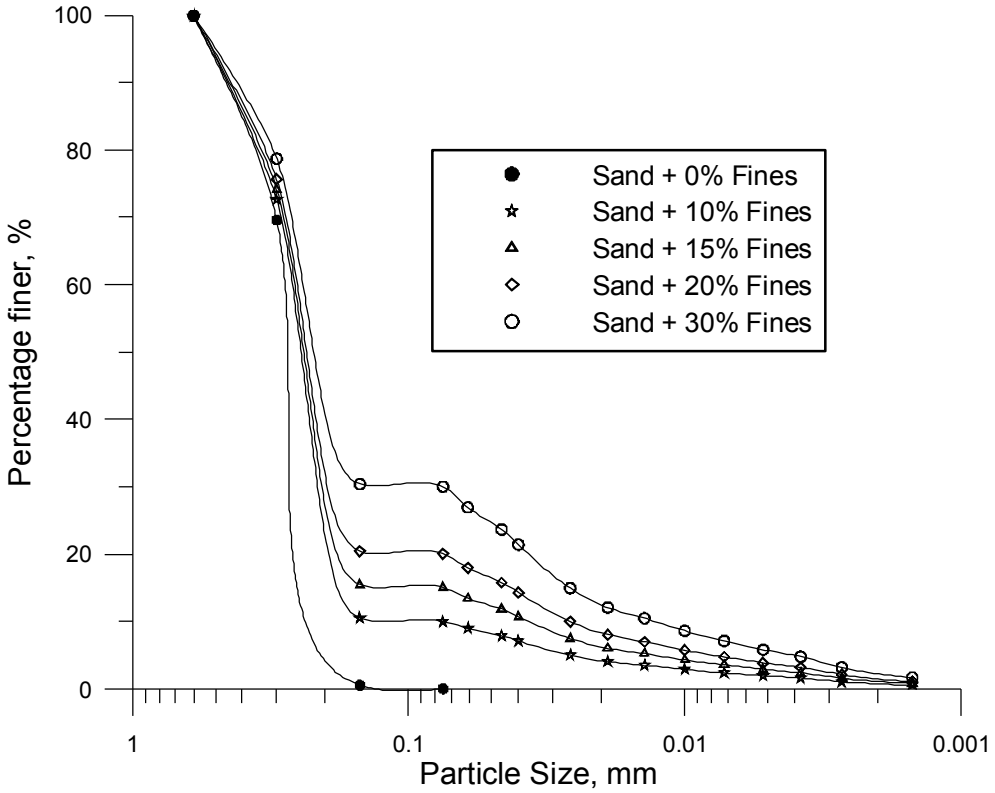

Figure 13. Grain size distribution curve of Sydney sand and Majura fines with Kaolin

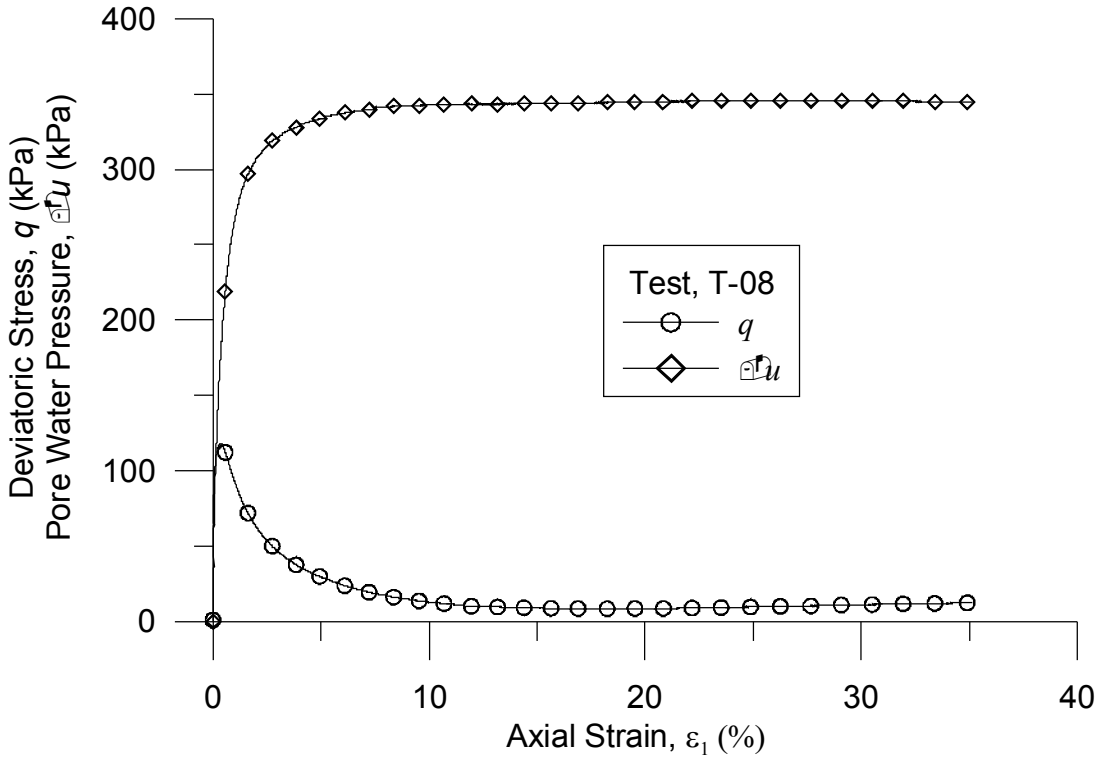

(a)

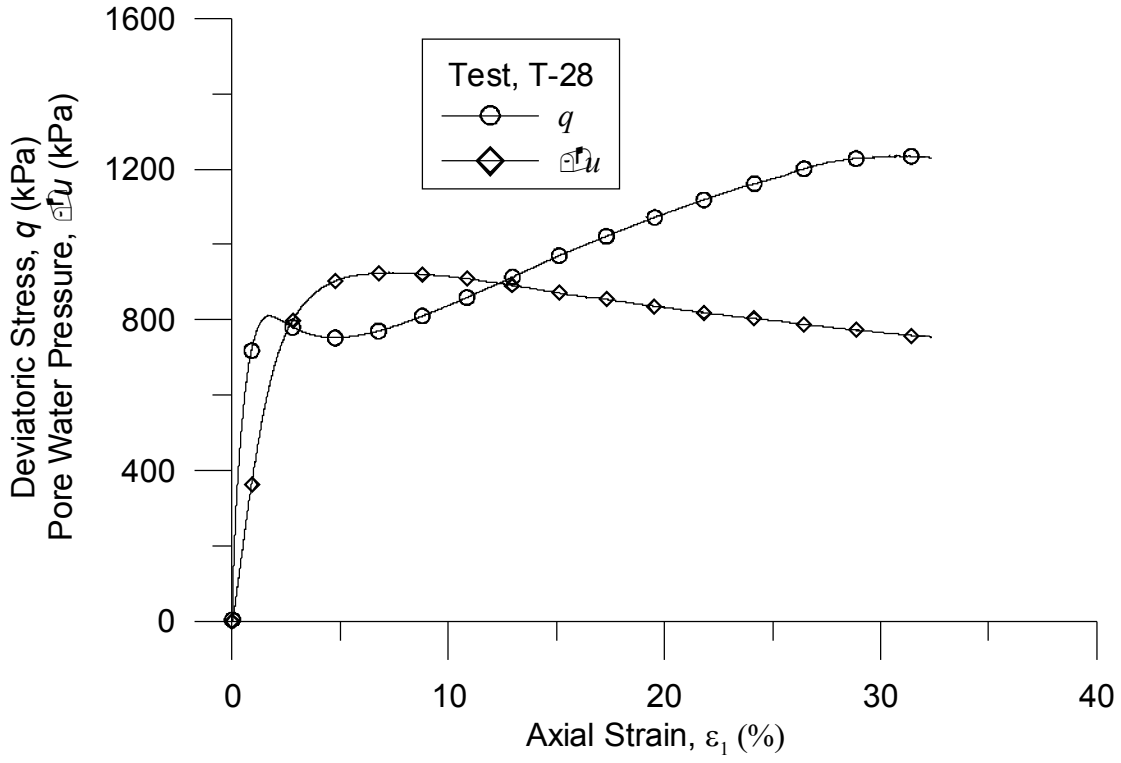

(b)

Figure 14. Pore water pressure and deviatoric stress response for (a) flow behaviour (test T-08) and (b) limited flow behaviour (test T-28)

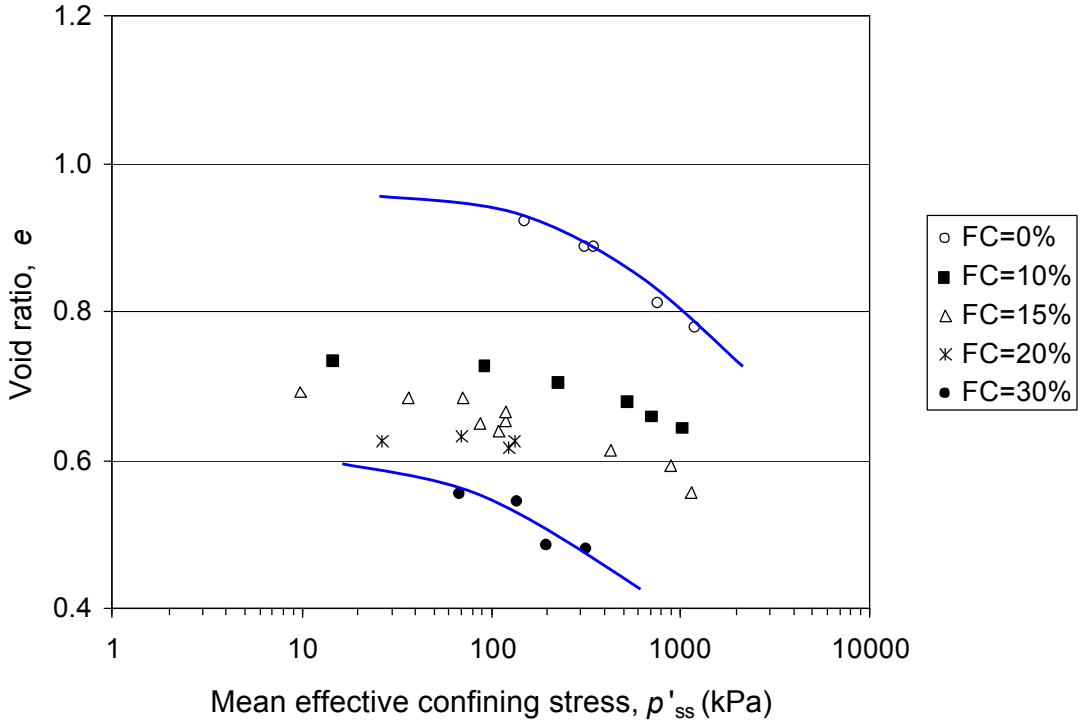

Figure 15. Multiple SSLs for Sydney sand with different fines content

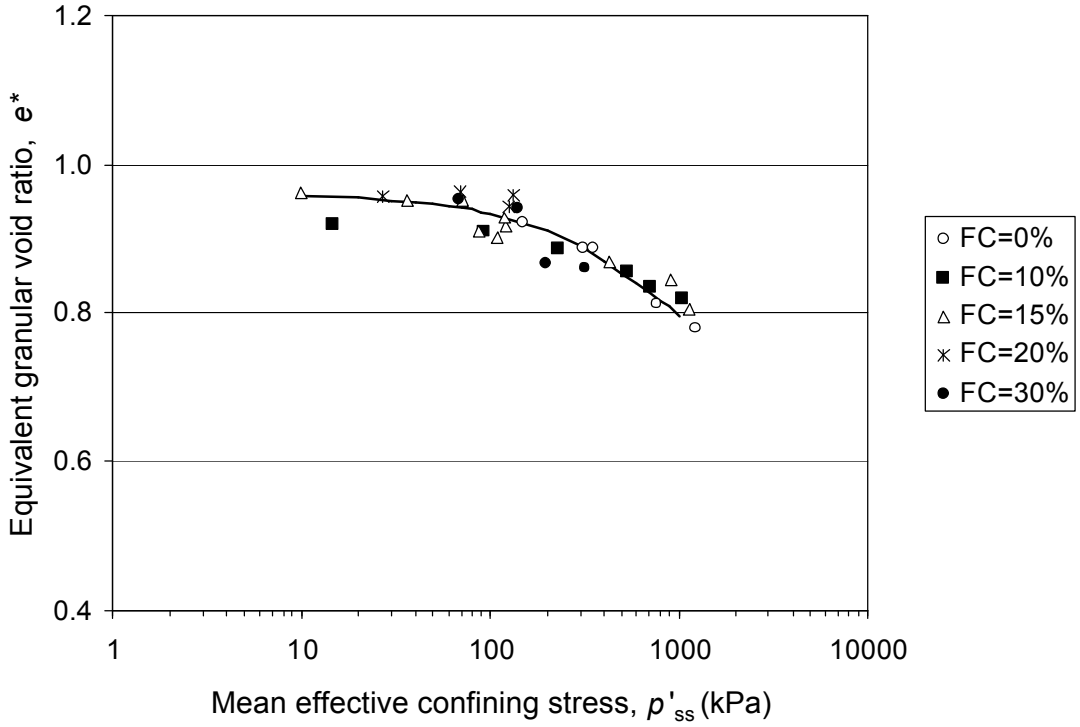

Figure 16. A unique equivalent granular SSL for Sydney sand with different fines content

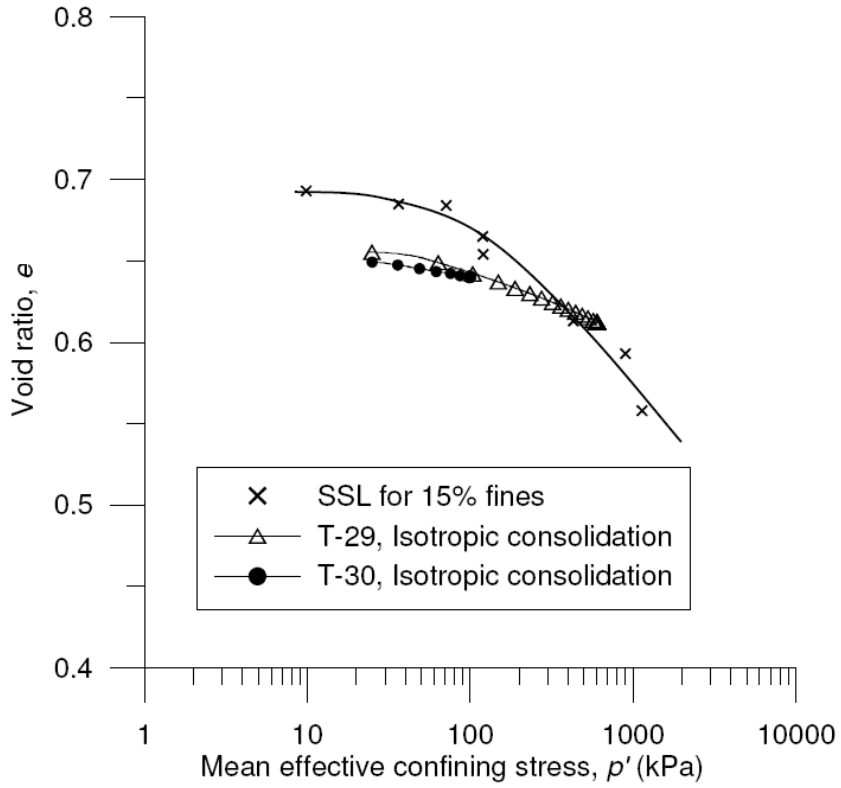

Figure 17. Consolidation line of tests T-29, T-30 and SSL for Sydney sand with 15% fines

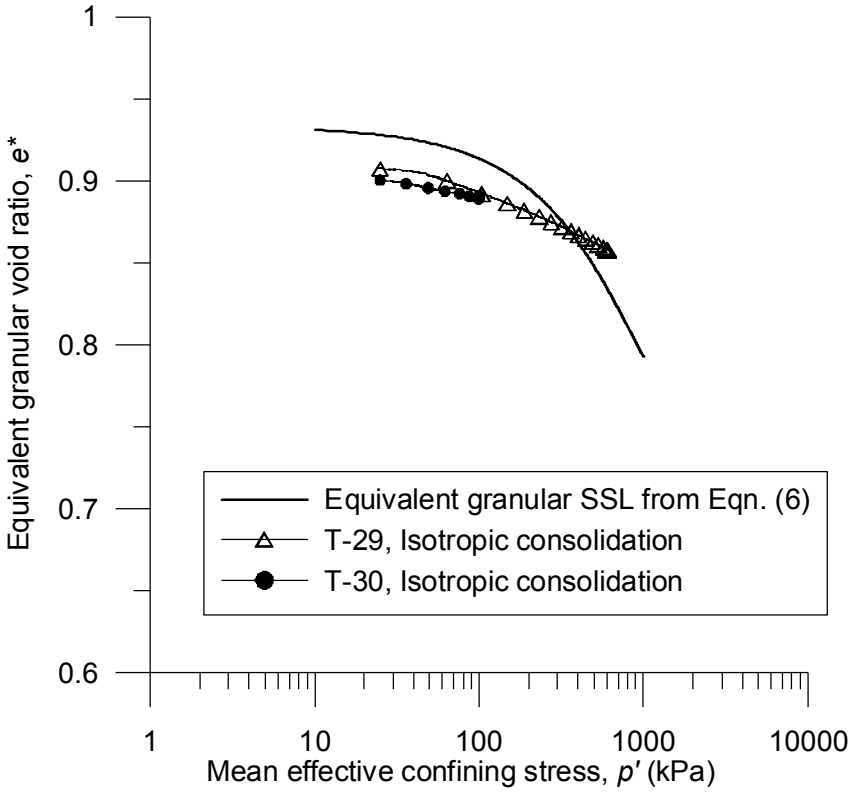

Figure 18. Consolidation line and unique SSL of T-29 and T-30 (Sydney sand with 15% fines)